

Study of Plasma and Energetic Electron Environments and Effects

ESA contract 11974/96/NL/JG(SC)

WP 130 TECHNICAL NOTE (SPEE-WP130-TN)

Version 2.0
February 22, 1999

Analysis of Freja Charging Events: Statistical Occurrence of Charging Events

Prepared by

J-E. Wahlund, L. J. Wedin, T. Carrozi, A. I. Eriksson, and B. Holback,
Swedish Institute of Space Physics, Uppsala Division

L. Andersson
Swedish Institute of Space Physics, Kiruna Division

H. Laakso
Finish Meteorological Institute, Helsinki

ESA Technical Officer: A. Hilgers, Space Environments and Effects Analysis Section (TOS-EMA)
ESA Technological Research Programme, Space Environments and Effects Major Axis

TABLE OF CONTENTS

2	Introduction	3
2.3	Purpose of document	3
2.4	Related documents	3
2.5	The need for statistical prediction of spacecraft charging	3
3	Experimental Constraints of this Study	5
3.3	Freja orbit and attitude	5
3.4	General on Freja data taking	5
3.5	Instrumental restrictions and possible error sources	5
3.5.1	MATE data	5
3.5.2	TESP data	5
3.5.3	TICS data	6
3.5.4	Langmuir Probe data	6
3.5.5	Plasma Wave data	7
3.6	Selection criteria for Freja charging events	7
3.7	Determination of plasma density	7
3.8	Determination of sunlight conditions	7
3.9	Normalisation of the statistical data	9
4	The Results of the Statistical Study	16
4.3	Amount of data and charging characteristics	16
4.4	Variation with sunlight conditions	18
4.5	Variation with geomagnetic location	19
4.6	Variation with geomagnetic activity	23
4.7	Variations with the cold plasma characteristics	25
4.8	Variation with energetic particle characteristics	26
4.9	Variation with altitude and magnetic field strength	30
5	Discussion of Results	32
5.3	Characteristics of Freja Charging events	32
5.4	Comparison with DMSP Statistics	33
6	Conclusions & Guidelines for Future Missions	34
7	References	35

1. INTRODUCTION

1.1. PURPOSE OF DOCUMENT

This document presents the results provided by work package WP130, *Analysis of Freja Charging Events/Statistical Occurrence of Charging Events*. This work package includes a statistical study based on all the data from the Freja spacecraft sampled within the time period October, 1992, to April, 1994 during declining solar activity conditions. It is used to establish the occurrence and intensity characteristics of surface charging events from this polar (high latitude) orbiting spacecraft in the altitude range 1000 - 1800 km. The Freja satellite had a highly advanced plasma payload package suitable for spacecraft charging studies, and it was especially designed to be as electrically clean as possible. Despite the high conductivity of the surface materials (see SPEE-WP120-TN) and the favourable secondary electron characteristics of the dominant Indium Tin Oxide (ITO) surface coating, numerous charging events did indeed occur with negative charging levels as large as -2000 Volts. Charging should therefore be of concern for future spacecraft designers. The statistics is complemented with information on the environmental characteristics during the charging events, such as cold plasma density, energetic electron and ion distributions, light conditions, and geomagnetic location as well as geomagnetic activity. The study is complemented with a comparison with previously made spacecraft charging studies.

The work package also provides a detailed database of the Freja charging cases accessible by the SPEE WWW server (<http://www.geo.fmi.fi/spee>). The database include all the 291 charging events found in the Freja dataset. This database can be used for further studies of surface charging on the Freja spacecraft, but its primary aim is to provide an easy accessible database on environmental statistics for spacecraft charging. The SPEE WWW server is described in the *User and Software Requirements Document* to work package WP330 [SPEE-WP330-URD/SRD].

1.2 RELATED DOCUMENTS

The following documents are included in work package **WP100**, Analysis of Freja Charging Events:

- SPEE Final Summary Report
- Charging Events Identification and Case Study of a Subset of them [SPEE-WP110-TN]
- Modelling of Freja Observations by Spacecraft Charging Codes [SPEE-WP120-TN]
- Statistical Occurrence of Charging Events (this document) [SPEE-WP130-TN].

1.3 THE NEED FOR STATISTICAL PREDICTION OF S/C CHARGING

Electrical charging of the surface and internal structure of spacecrafts have been found to cause operational problems to the spacecrafts themselves as well as their on-board instrumentations. Examples of payload measurement problems are also evident in this statistical study as well as in the detailed study of Freja charging events (SPEE-WP110-TN). When the resulting electric field exceeds the breakdown field intensity for a material, an electrostatic discharge occurs. Electrostatic arcs are believed to be responsible for a large part of spacecraft anomalies including command errors, phantom commands, degraded sensor performance, parts failure, and even complete loss of spacecraft missions (see e.g. *Anderson and Koons*, 1996; *Garret*, 1981; *Garret and Pike*, 1980; *Leach and Alexander*, 1995; *Koons and Gorney*, 1991). It is therefore of outmost importance to investigate in what space regions, and with what physical mechanisms and effects, high levels of spacecraft charging occur. Based on the knowledge of the electrical plasma environment expected for a specific spacecraft mission, a spacecraft design can be made to reduce harmful effects.

This study can be used for future prediction of spacecraft charging in the particular region around Earth where Freja traversed, i.e. high-latitude polar orbit in the altitude interval 1000 - 1800 km. Only very few studies of spacecraft charging have previously been carried out, and for this particular region only studies based on the Defence Meteorological Satellite Program (DMSP) data are available. This study is briefly compared to the DMSP statistics below, and the DMSP studies are discussed in more detail in SPEE-WP110-TN.

This study is probably more important as an attempt to identify the exact physical mechanisms behind charging and effects on spacecrafts in a more general way, since interplanetary travel is continuously targeted to new regions in space and since new propulsion methods based on electrical ion thrusters will become widely used. When these mechanisms are known, hazardous spacecraft charging and effects may be predicted in advance when certain environmental conditions (described herein) are thought to be encountered by a particular spacecraft. More information regarding spacecraft charging in general and its effects can be found in SPEE-WP110-TN.

2. EXPERIMENTAL CONSTRAINTS OF THIS STUDY

2.1 FREJA ORBIT AND ATTITUDE

The Freja spacecraft orbits Earth with a 63° geographic inclination, a perigee of 601 km above the southern hemisphere and an apogee of 1756 km above the northern hemisphere. This study is based only on the northern hemisphere data and the altitude coverage is therefore limited to 1000 - 1800 km. In consequence, Freja pass the auroral regions almost tangentially during each orbit (orbital period is 109 min). Freja is a spin-stabilized sun-pointing spacecraft with a spin period of about 6 seconds, and its structure and surface materials are presented in SPEE-WP120-TN. Freja was successfully launched on October 6, 1992, and many of the onboard instruments had stopped operating by late 1995 when the Freja mission ended. This study is limited to the time period October, 1992, to May, 1994, during a time when good plasma measurements were provided by most on-board instruments. This time period occurs during a declining phase of the solar cycle from medium solar activity to minimum solar activity.

2.2 GENERAL ON FREJA DATA TAKING

Data transmission to the ground occurred at Prince Albert (Canada) and Esrange (Kiruna, Sweden), which limited the coverage of high TM data taking to the northern hemisphere. Only low TM survey data are available from the southern hemisphere and consequently only limited information of charging events are available from this lower altitude part. This study therefore excludes all possible southern hemisphere Freja charging events, even though a few seems to have been found.

The Freja spacecraft contained 73 kg of state of the art plasma payload. For a description of all payload we refer to SPEE-WP110-TN and a special issue in Space Science Rev. (*Lundin et al.*, 1995). In the following only some characteristics of the payload relevant for this statistical study will be given.

2.3 INSTRUMENT RESTRICTIONS AND POSSIBLE ERROR SOURCES

2.3.1 MATE Data

The MAgnetic imaging Two-dimensional Electron spectrometer (MATE), measures electron energy and angular distributions in the energy range 0.1-100 keV. MATE consist of a 360° field-of-view sector magnet energy analyser with 90° deflection angle for simultaneous energy and pitch-angle determination. The sampling rate for the full energy range is 10 ms, and a collimator system enables measurements of the energy spectrum at 16 energies (with resolution $\Delta E/E = 30\%$), and 30 angular sectors.

Unfortunately, the MATE instrument was not deployed completely and was to 1/3 blocked by the Freja spacecraft itself and only every 4th angular sector have data. Also, the MATE instrument did only work properly up to orbits around 1600, whereafter only the integrated flux of the high-energy electrons (with some pitch-angle information) could be obtained after that. In addition, the lowest energy channels was found to give uncertain data. This instrument is otherwise the only instrument onboard Freja that could give accurate information on the high energy electrons.

2.3.2 TESP Data

The Two-dimensional Electron SPectrometer (TESP) on Freja consists of a "top-hat" style sweeping electrostatic analyser. The energy range of 20 eV-25 keV is covered in 32 sectors to complete a spectrum. Depending on instrument mode, 16 or 32 spectra are returned each second (31.25 ms

resolution). The angular field-of-view is the full 360° and electrons are counted in 32 equally spaced bins, yielding an angular resolution of 11° . The entrance aperture of the TESP also contains a set of electrostatic deflectors which allows the plane of acceptance to be "warped" into a cone.

The TESP experiment started working around orbit 720, when the instrument software were sent to the spacecraft after the launch. The TESP data covers only energies up to 25 keV, but give nevertheless important information regarding the high-energy electrons. Since low energy electrons may cause an excess emission of secondary electrons (and thereby mitigate charging), the information from this experiment is very useful. Note though that the energy channels below about 30 eV was found to give uncertain data. Finally, the TESP data used in this particular statistical study made use of the "overview" analysed data where errors up to a factor 3 in the electron flux may exist. This is not the case for the TESP data presented in SPEE-WP110-TN.

2.3.3 TICS Data

The Three-dimensional Ion Composition Spectrometer (TICS) measures the positive ion distributions in the energy range 0.5 eV/q - 5 keV/q . TICS carry out measurements perpendicular to the spacecraft spin plane and thus gives 3D ion measurements every 3 s. TICS consists of a spherical "top-hat" electrostatic analyser with 16 or 32 energy steps sampled each 10 ms. This means that one 16 step energy sweep takes $160 \text{ ms} + 40 \text{ ms}$ for adjusting the high voltage. TICS also gives limited ion composition information in the range $1\text{-}40 \text{ amu/q}$. This instrument gives the best measurement of the degree of negative charging, since the whole ion population is accelerated toward the spacecraft (and TICS) and will be detected at energies corresponding to the potential of the spacecraft. Even as small negative potentials as -5 V can be seen in the TICS data.

2.3.4 Langmuir Probe Data

There exist 4 possible spherical Langmuir probes (P3-P6) situated on wire booms, and a cylindrical Langmuir probe (CYLP) onboard Freja. The CYLP is almost always available, but the operation of the spherical Langmuir probes (LP) depends on the measurement mode for a certain orbit in question. The spherical LP's are 6 cm in diameter and coated with graphite (DAG 213). They are situated 5.5 m (P5 and P6) and 10.5 m (P3 and P4) from the spacecraft respectively. The CYLP is 57 cm long and 1 cm in diameter, and is made of carbon fibre. It is mounted on the DC magnetometer stiff boom (2 m from the spacecraft) parallel to the spin axis. As the spin axis is "sun-pointing" within 30° , this will minimise the projected surface area and thus the photoelectron emission. The CYLP data is not used in the statistical study because of difficulties in interpreting (correctly modelling) the results from this probe.

A Langmuir probe samples all current contributions in a plasma at a certain biasing potential, with respect to the spacecraft floating ground, according to its current-voltage characteristics. Therefore, a LP is a direct measurement of the charge state of the probe (and spacecraft). Most often this fact gives information on the density and electron temperature of the ambient thermal plasma, since the sampled probe current usually is directly proportional to $n_e / \sqrt{T_e}$ and because the ambient thermal electron current usually dominates the current collection for positive probe potentials. However, when the spacecraft (and probe) attains a large negative potential (i.e. a large negative charge) with respect to the surrounding plasma, the thermal electrons will start to be repelled from the LP. If the negative potential becomes much larger than the average energy of the thermal electrons (typically below 2 eV), a majority of these electrons cannot easily reach the negatively charged LP, and the probe current drops sharply to the very low values more characteristic for the collected ion thermal current. A LP current below $5 \cdot 10^{-8} \text{ A}$ therefore either indicates a negative charging event of at least a few Volts negative (it is biased -8 V with respect to the spacecraft), or a very low electron density below 10^7 m^{-3} . The sampled LP current is therefore a very sensitive measurement for spacecraft charging, even though it does only give a threshold value for the negative potential during high level charging events.

2.3.5 Plasma Wave Data

The plasma wave experiments (F4) did measurements in basically three frequency regimes, LF (5-2000 Hz), MF (5 Hz-16 kHz) and HF (10 kHz-4 MHz). Only the HF measurements were used in this statistical study for an accurate determination of the plasma density (see below). All the wave measurements were normally made in snapshots of various lengths and duty cycle, depending on sampling rate, telemetry allocations, etc. The HF measurements were either made with the P1-P2 probe pair (21 m) in the spacecraft spin plane, or by a special short (1.2 m) antenna probe pair (PAB) mounted on one of the magnetometer booms. All signals were transmitted to the ground as waveforms and there is no onboard treatment except filtering, A/D conversion and intermediate storage.

2.4 SELECTION CRITERIA FOR FREJA CHARGING EVENTS

A detailed discussion of possible selection criteria for Freja charging events can be found in WP110 [SPEE-WP110-TN]. Unfortunately, this very detailed selection is not practical when applied to the huge Freja database as a whole. Instead a somewhat modified and automatic procedure was invoked to identify Freja charging events. The following process was carried out when selecting charging events for this statistical study:

- All occasions when all available Langmuir probe currents dropped below $2 \cdot 10^{-8}$ A was considered possible charging events. This resulted in some 500 possible events.
- All these events were then checked "by eye" in the TICS data for a lifted (in energy) ion distribution at all pitch angles.
- If these events had an anomalous correspondence in the electron density, as inferred from the HF plasma emissions (F4 data) and the Langmuir probe current data, they were considered to be charging events.
- All events with a charging level above about 5 V were kept in the database.

The above procedure resulted in a total of 291 charging events up to orbit 7000 (October, 1992 to April, 1994).

2.5 DETERMINATION OF PLASMA DENSITY

The HF plasma wave emissions were used to determine the electron density during each of the charging events. The estimates are based on either the narrow-band Langmuir emissions or the upper cutoff frequency of the electrostatic whistler type waves as described in SPEE-WP110-TN.

2.6 DETERMINATION OF SUNLIGHT CONDITIONS

The sunlight conditions for each event in this study were determined from the geometric considerations when the Sun was over the limb of Earth from a Freja viewpoint. These are in good agreement with the UV photometer data from Freja. All sunlight and terminator events in the database where photometer data was available were checked (orbits 1800 - 9400). This included 18 sunlit events and 8 terminator events. A few of the events are presented below, where the rest of the data can be found on the SPEE WWW server (<http://www.geo.fmi.fi/spee>).

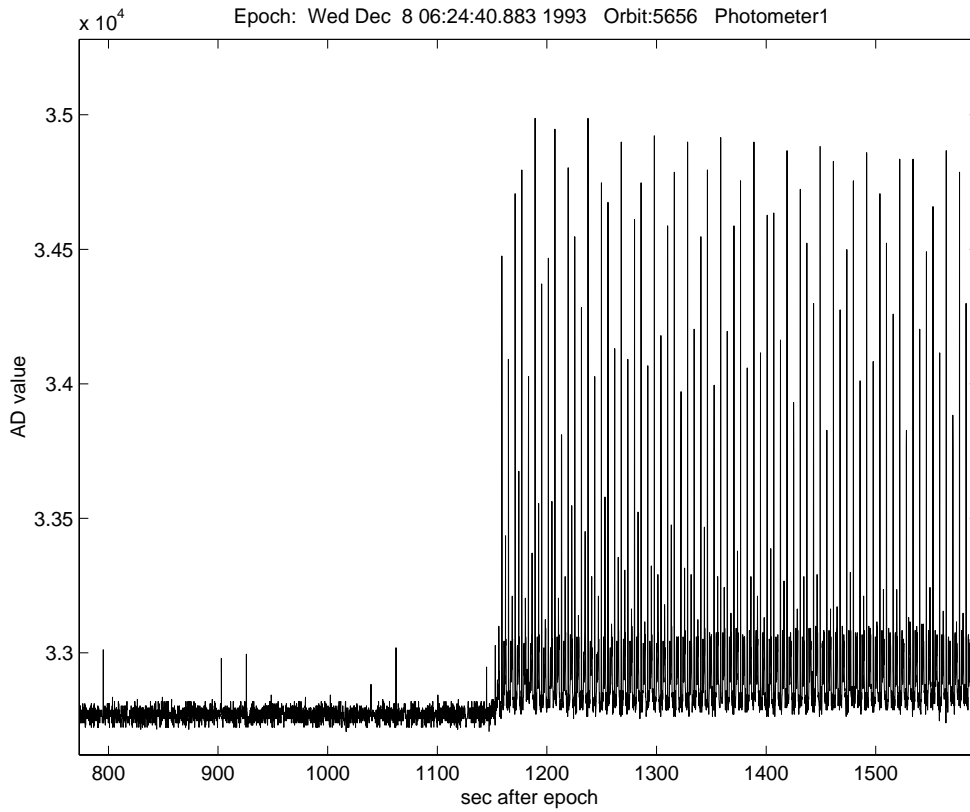


Fig 2.6.1: Orbit 5656 had two charging events reaching -20 V to -50 V at 06.41:20 UT (1000 s) in eclipse and at 06.47:20 UT (1360 s) in sunlight.

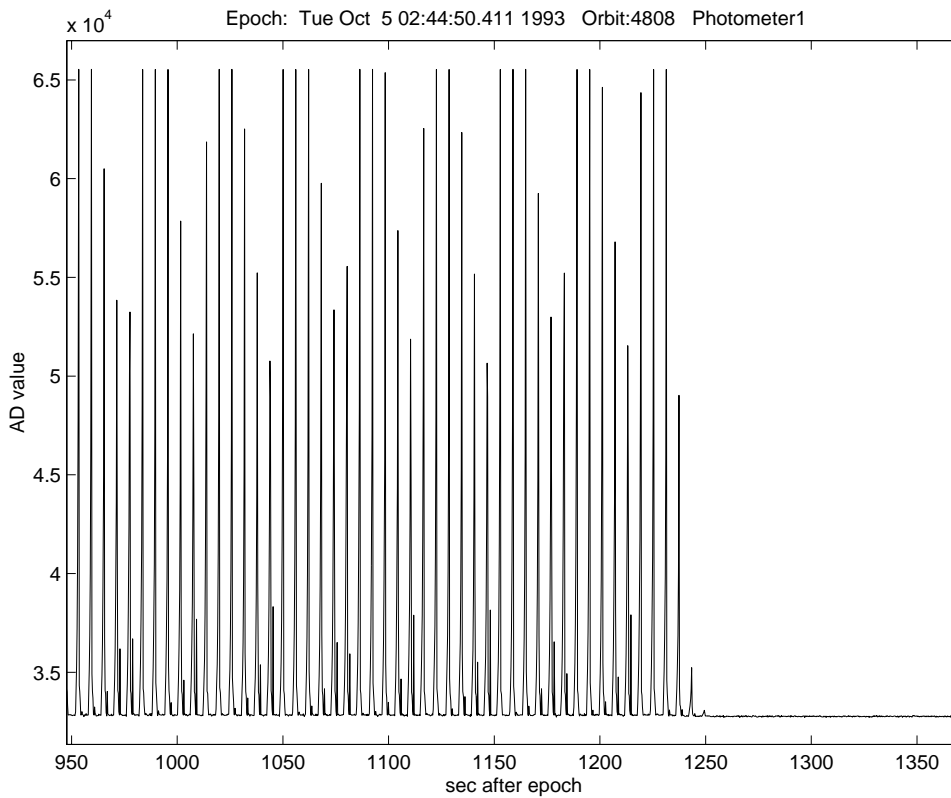


Fig 2.6.2: Orbit 4808 had one sunlight charging event to -50 V at around 03.03:20 UT (1110 s).

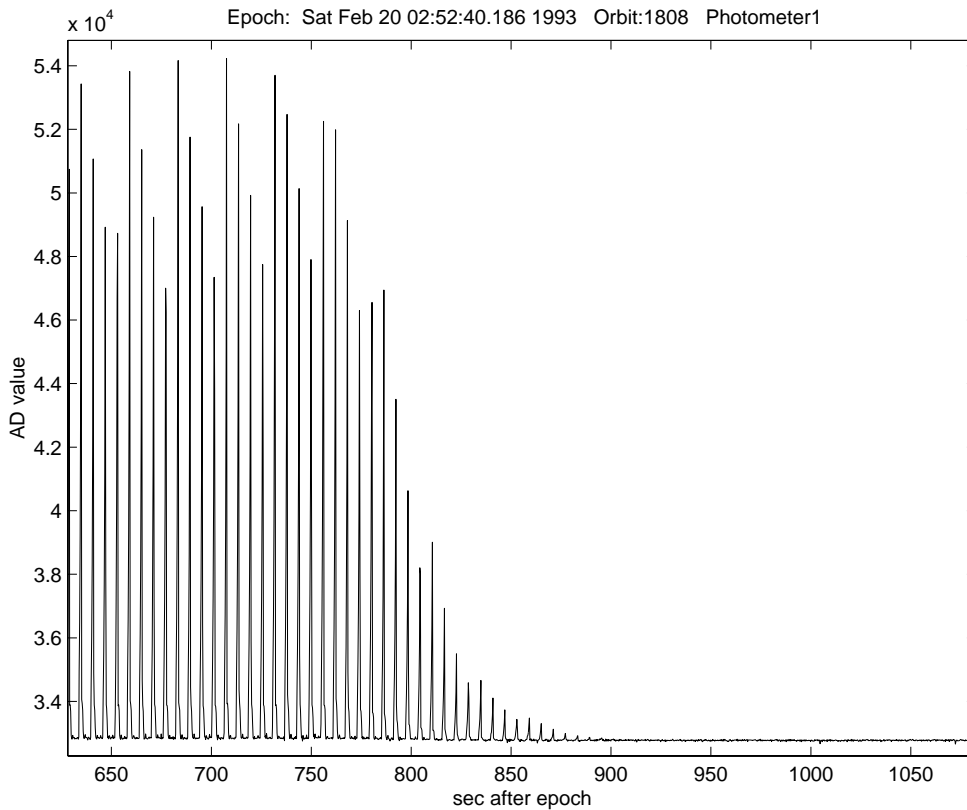


Fig 2.6.3: Two terminator low level charging events occurred near around 03.06:10 – 03.06:50 UT (810 – 840 s).

2.7 NORMALIZATION OF THE STATISTICAL DATA

All ephemerid data up to orbit 10,000 were used for normalisation of the statistical data. Five evenly distributed times where data existed were selected from each orbit. From these times orbit number, date, altitude, corrected geomagnetic latitude (CGLAT), magnetic local time (MLT), longitude and universal time (UT) were extracted. Only occasions where real data existed was kept for the normalisation.

Altitude Normalisation Data are presented in Figures 2.7.1 and 2.7.2. Fairly good altitude coverage exists down to around 1500 km, while only very few data exist down to about 1000 km. This is due to the high altitude northern hemisphere coverage by the Prince Albert and Esrange receiver stations. The low altitude survey orbits were mostly carried out after orbit 5000 and are not used in this study.

Altitude Coverage of FREJA

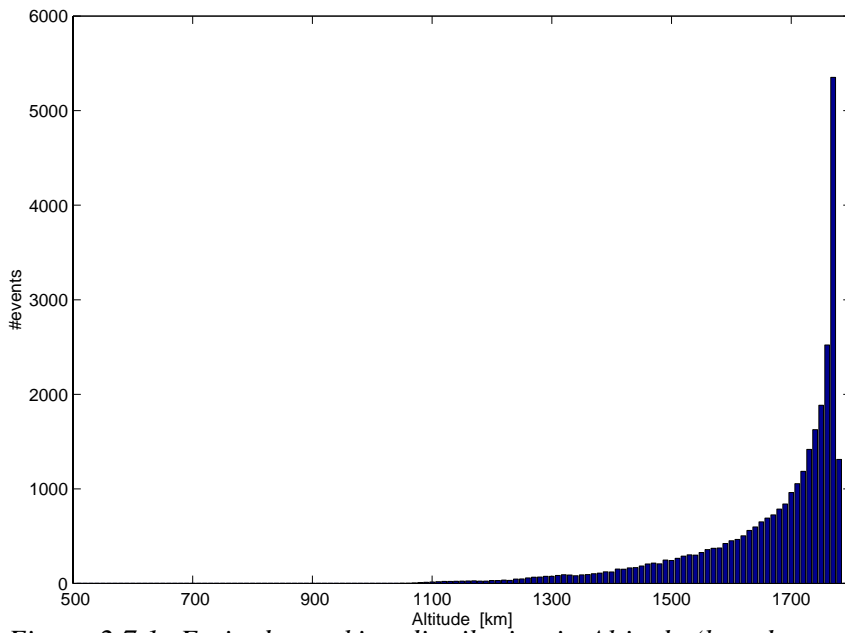


Figure 2.7.1: Freja data taking distribution in Altitude (based on orbits up to 10,000).

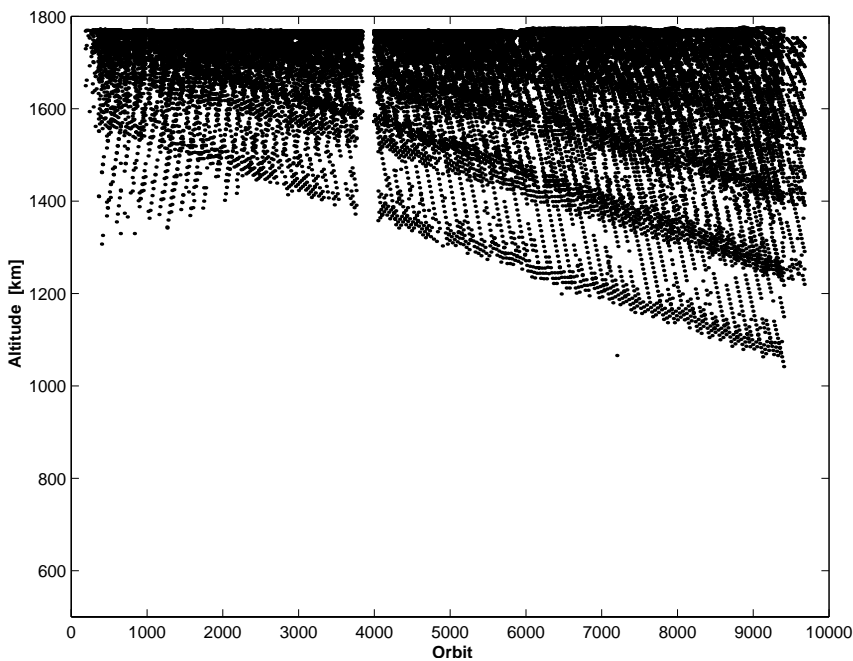


Figure 2.7.2: Freja data taking, Altitude vs time (orbit).

Corrected Magnetic Latitude Data are presented in Figures 2.7.3 and 2.7.4. The used Freja data covers the geomagnetic latitude interval $35^\circ - 75^\circ$, with no coverage elsewhere. The low altitude survey orbits cover the interval from -20° to -75° , but are not used in this study.

CG-Latitude Coverage of FREJA

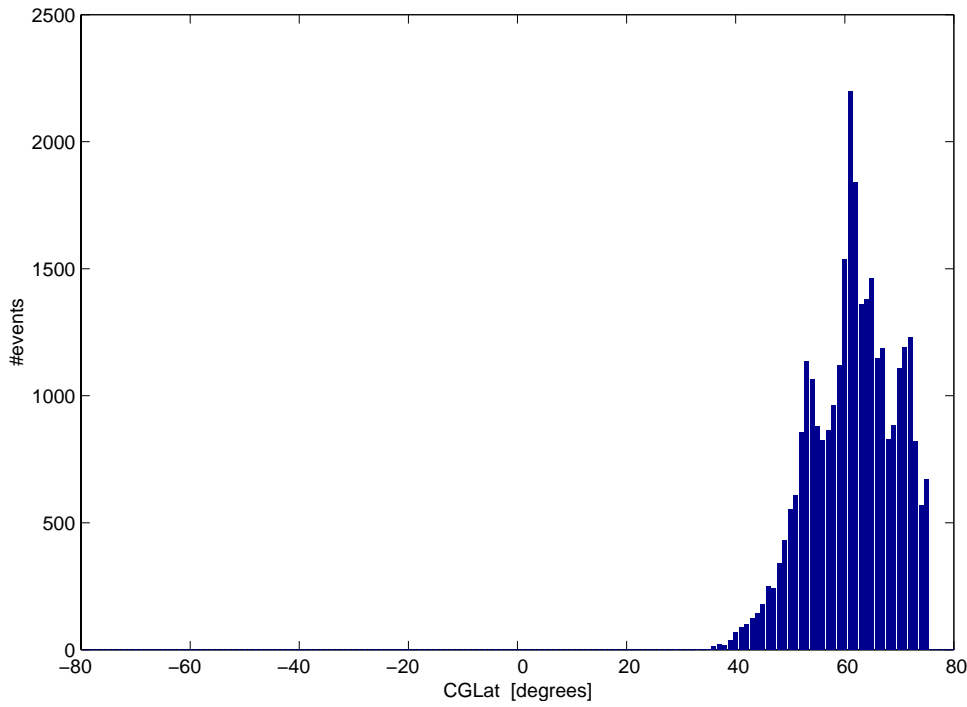


Figure 2.7.3: Freja data taking distribution in CGLAT (based on orbits up to 10,000).

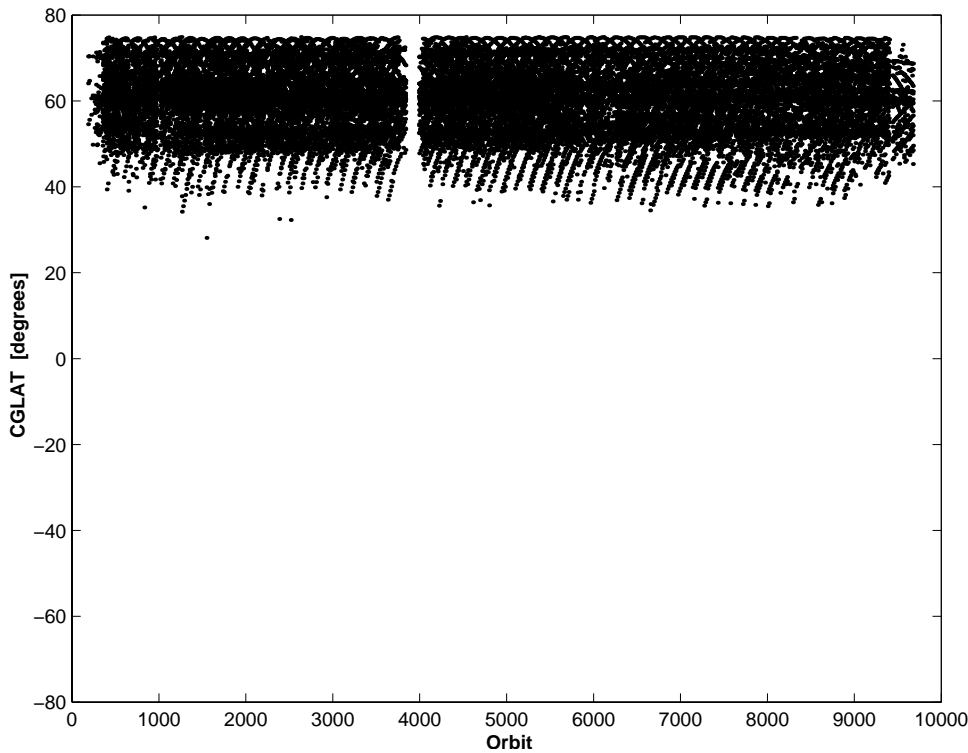


Figure 2.7.4: Freja data taking, CGLAT vs time (orbit).

Magnetic Local Time Data are presented in Figures 2.7.5 and 2.7.6. Freja covers all magnetic local times evenly.

MLT Coverage of FREJA

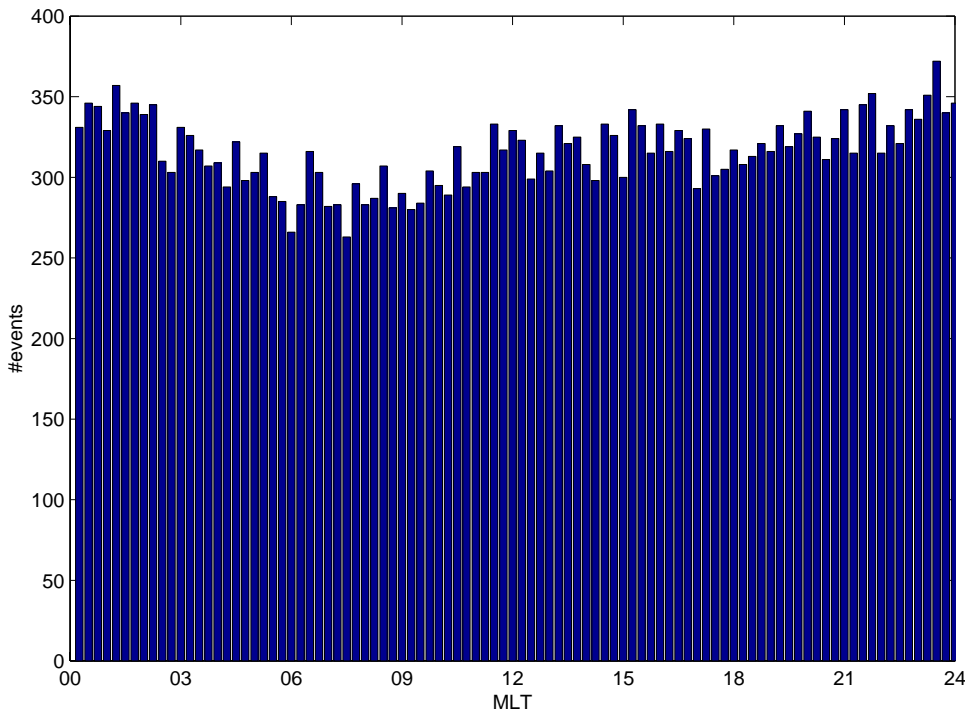


Figure 2.7.5: Freja data taking distribution in MLT (based on orbits up to 10,000).

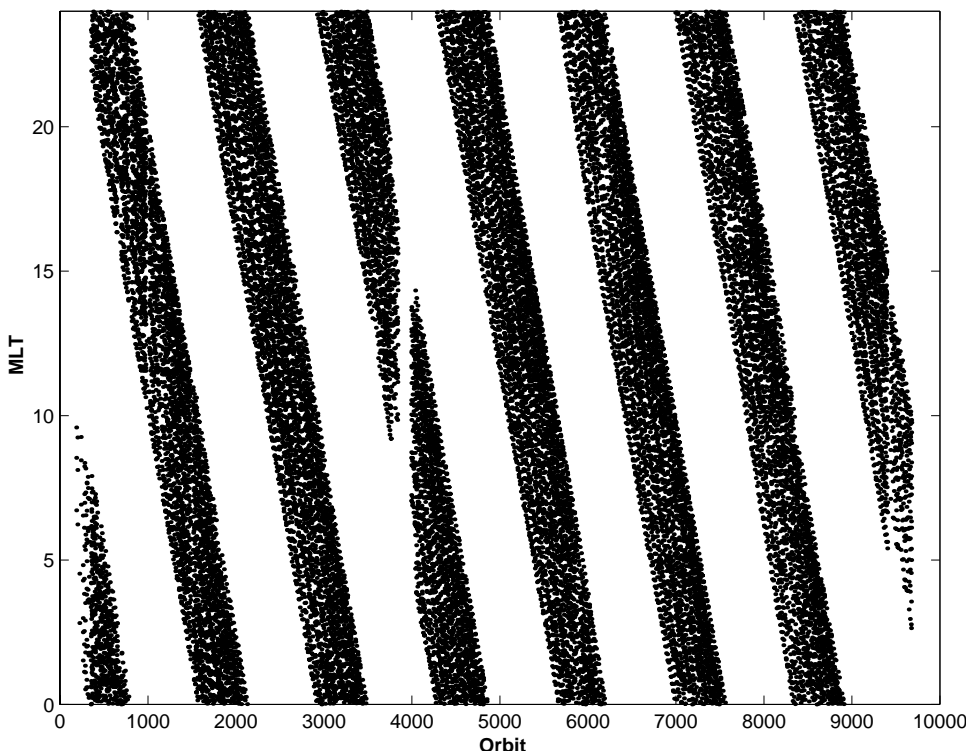


Figure 2.7.6: Freja data taking, MLT vs time (orbit).

Longitude Data are presented in Figures 2.7.7 and 2.7.8. The good longitude coverage between -150° and -45° reflects the increased telemetered data above the Prince Albert station (53° N, 106° W), while the good longitude coverage between -45° and $+90^\circ$ reflects the location of the Esrange receiver station near Kiruna in northern Sweden.

Longitude Coverage of FREJA

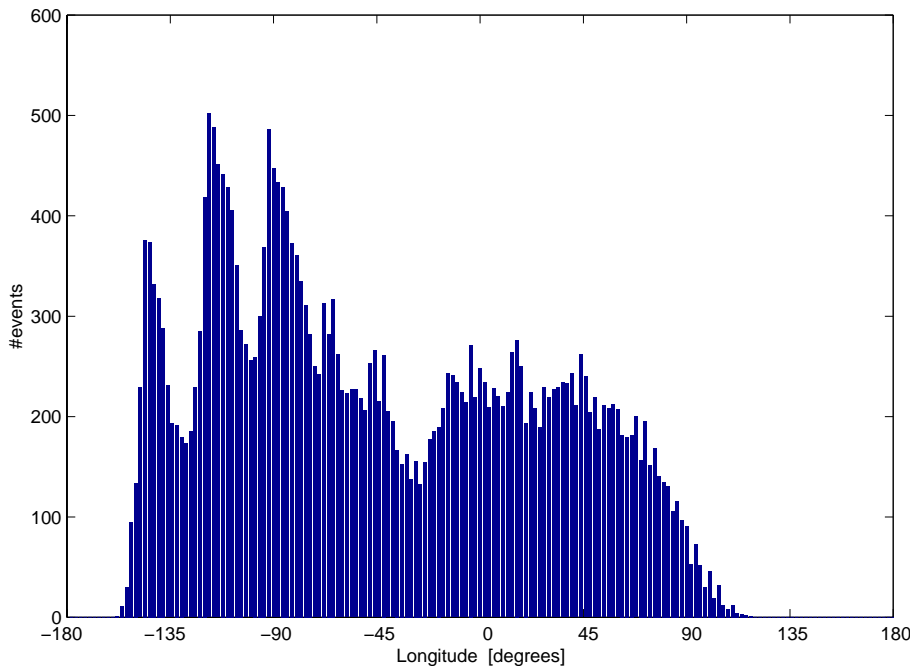


Figure 2.7.7: Freja data taking distribution in Longitude (based on orbits up to 10,000).

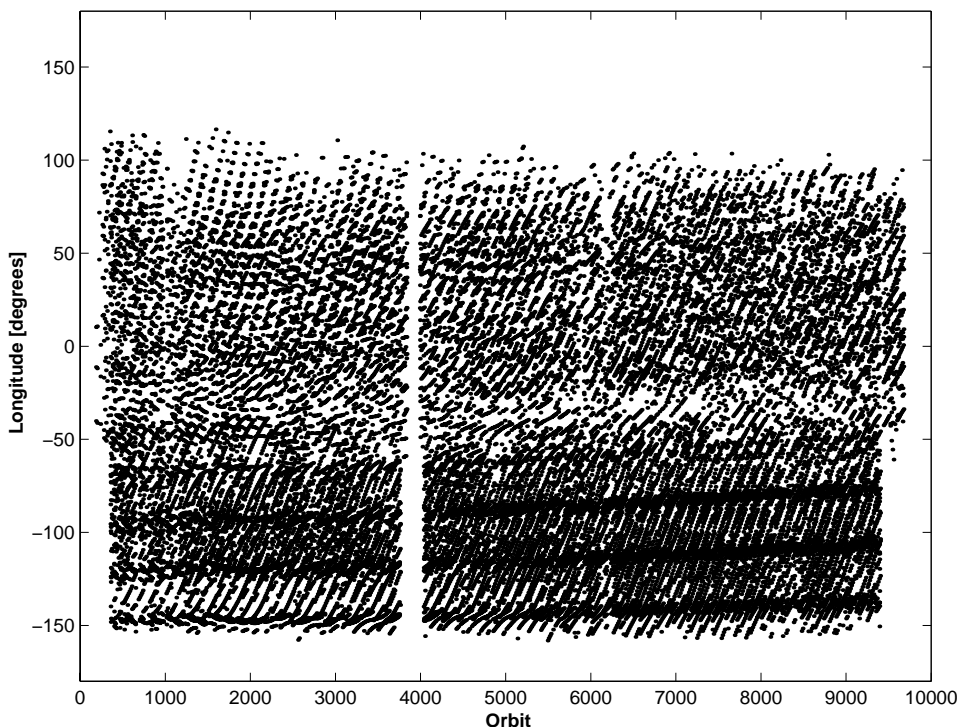


Figure 2.7.8: Freja data taking, Longitude vs time (orbit).

The Freja spacecraft orientation angle versus the geomagnetic field is presented in Figures 2.7.9 to 2.7.11. The magnetic field angle to the spacecraft spin axis is covered increasingly up to about 135° . The low coverage below 45° is due to a latitude effect (see Figure 2.7.11).

Spin-Axis Angle to Bz Coverage of FREJA

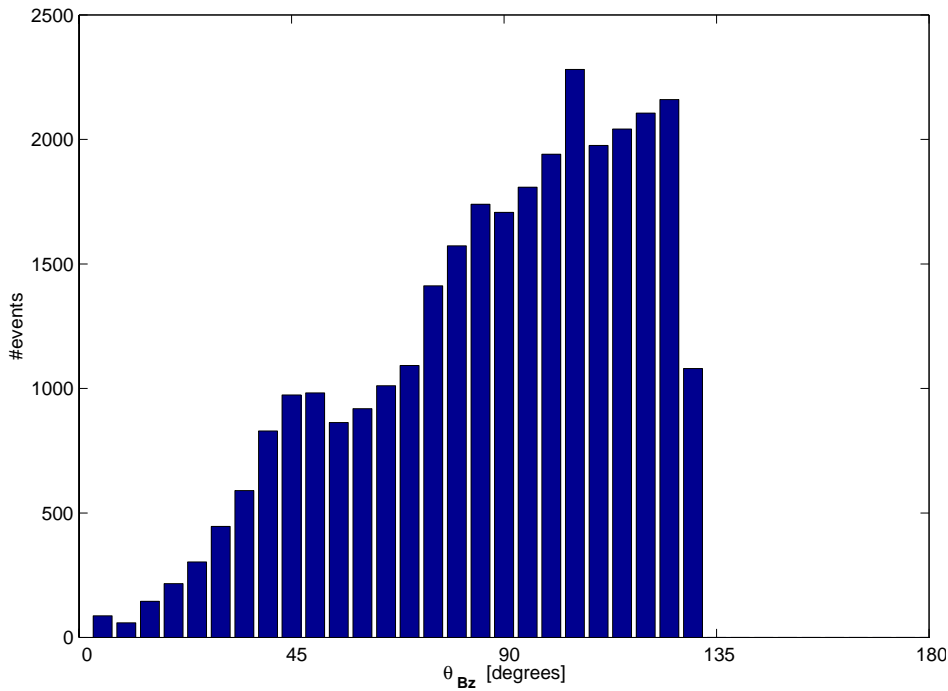


Figure 2.7.9: Freja data taking distribution in spin-axis angle to B (based on orbits up to 10,000).

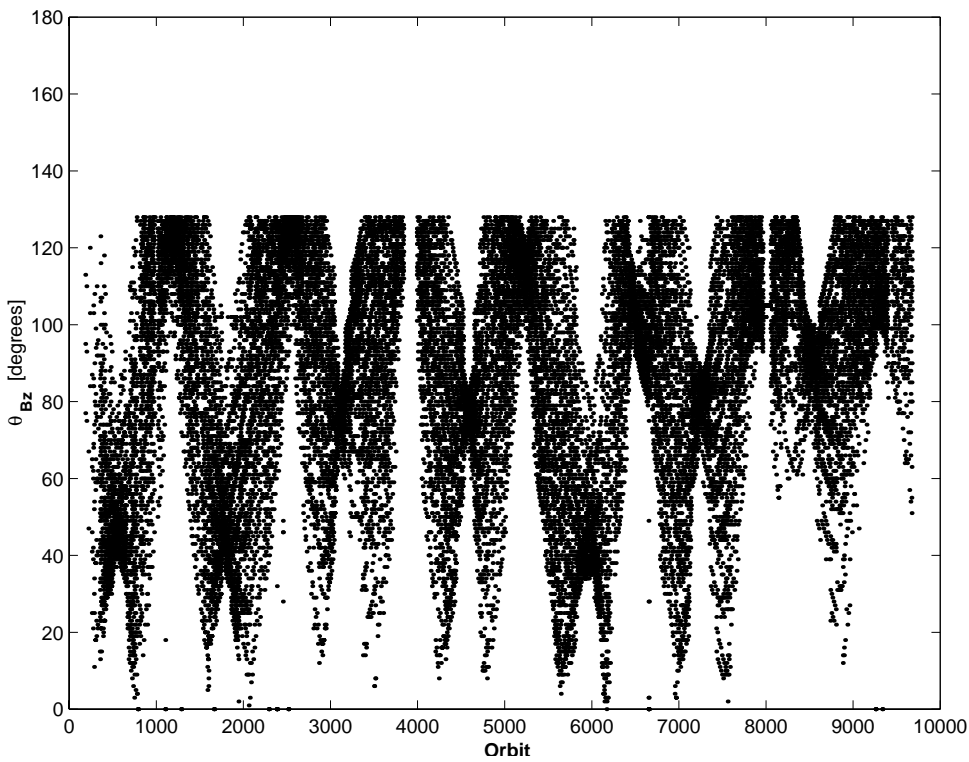


Figure 2.7.10: Freja data taking, spin-axis angle to B versus time (orbit).

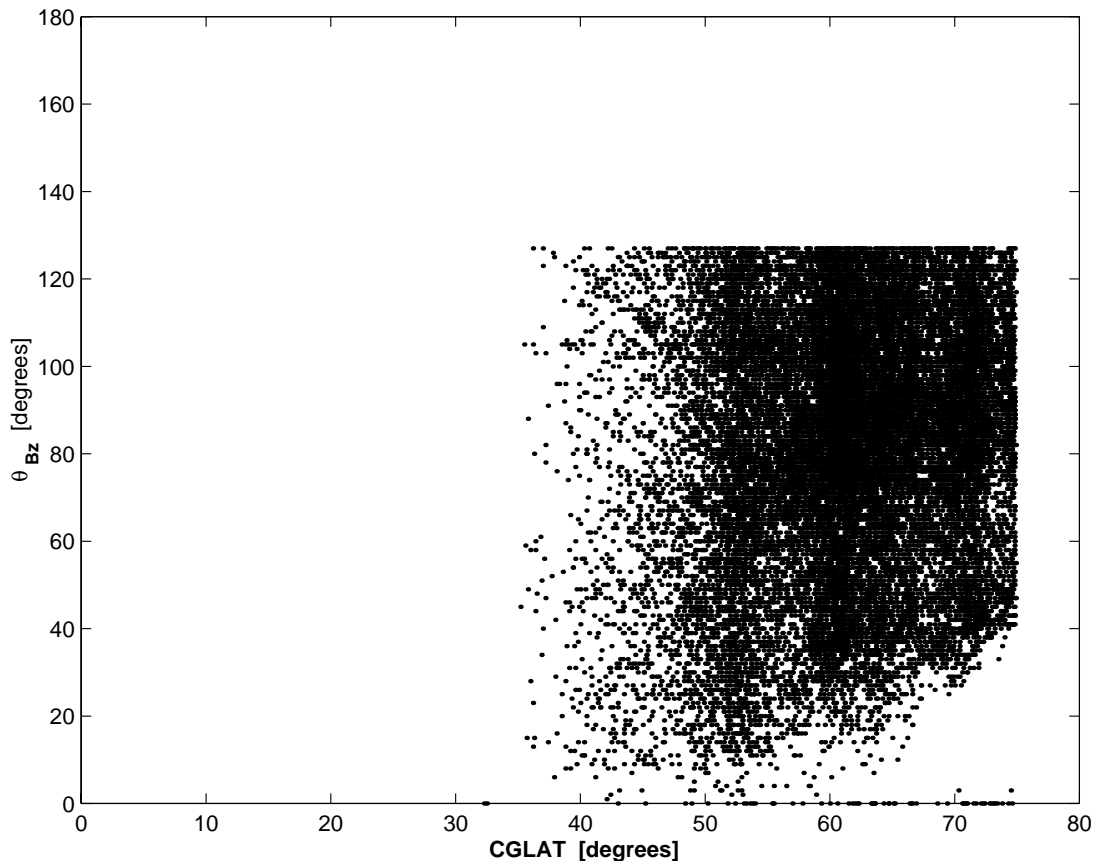


Figure 2.7.11: Freja data taking, spin-axis angle to \mathbf{B} versus CGLAT.

3. RESULTS OF THE STATISTICAL STUDY

3.1 CHARGING OCCURRENCE CHARACTERISTICS

This statistical study includes 291 charging events found in the time period October, 1992, to April, 1994. The main part of these events are low level charging events, i.e. peak charging below 10 V negative, as can be seen in Figure 3.1.1. However, a few of the Freja charging events reach higher negative charging levels than -2000 V. The duration of the main part of the Freja charging events (Figure 3.1.2a) are shorter than one minute, but some few last for a couple to several minutes. For charging levels above 10 V, there seems to be a preferred duration of about 20 seconds (Figure 3.1.2b). The duration of charging events reflect the time it takes Freja to traverse the auroral inverted-V structures, i.e. the high energy electron precipitation regions (see SPEE-WP110-TN).

The charging levels are 2-3 times larger than those reported from the F6 and F7 spacecraft within the Defence Meteorological Satellite Program (DMSP) traversing an altitude of 840 km (see e.g. *Gussenhoven et al.*, 1985; *Stevens and Jones*, 1995). This is somewhat remarkable, since the Freja spacecraft was designed to be as conductive as possible with an ITO coated surface and therefore should be much harder to charge. On the other hand, Freja traversed higher altitudes and therefore lower plasma density regions, a physical parameter which have been suggested to be of importance for surface charging (*Frooninckx and Sojka*, 1992). Also, the Freja charging levels are well below the maximum charging levels detected on spacecrafts in geosynchronous orbit, such as the AST-5, AST-6 and the SCATHA (P78-2) satellites (e.g. *Mullen et al.*, 1986; *Olsen*, 1983), where charging levels of several thousands of Volts are readily achieved.

Charging Level of FREJA Charging Events

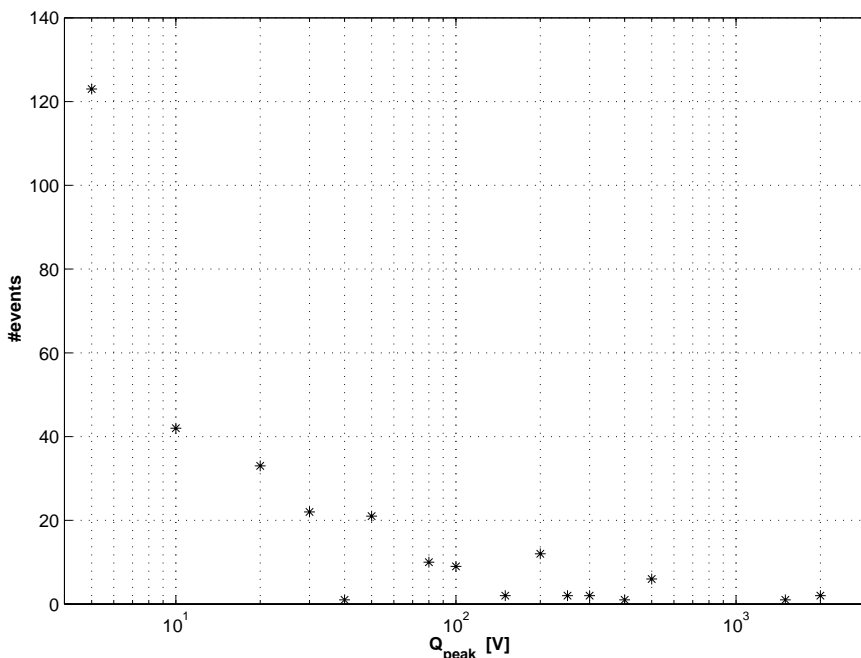


Figure 3.1.1: Distribution of charging levels. Negative charging levels in excess of -2000 V are detected, but most events have charging levels below 100 V negative.

Duration of FREJA Charging Events

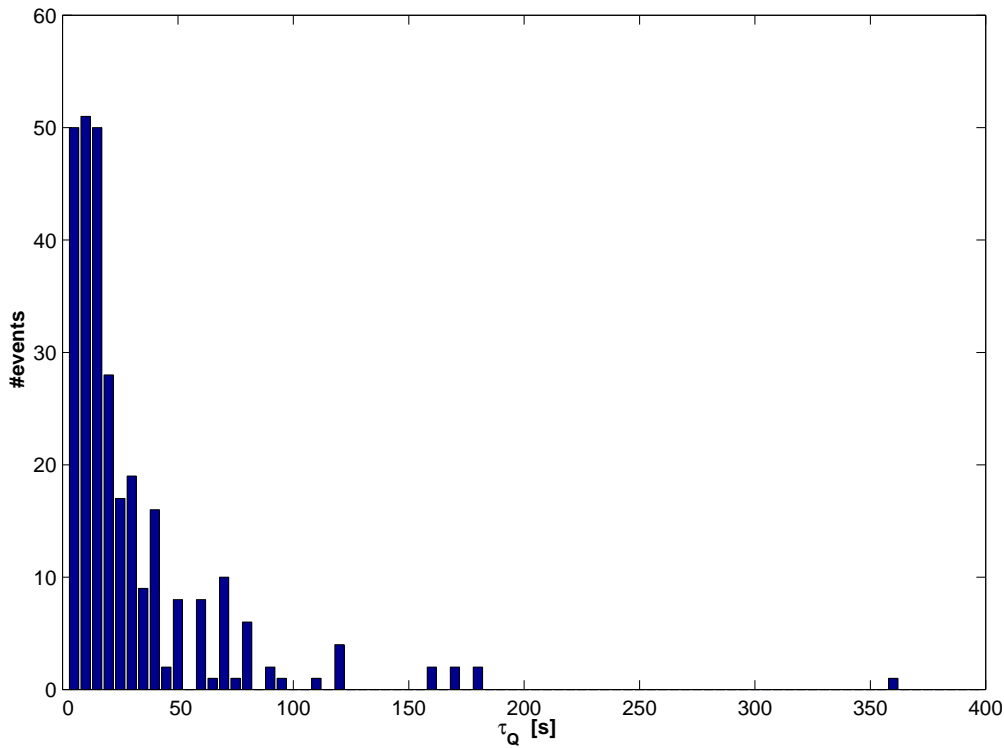


Figure 3.1.2a: Distribution of time duration of charging events (incl. all 291 events). Most events have a duration of less than a minute.

Duration of FREJA Charging Events

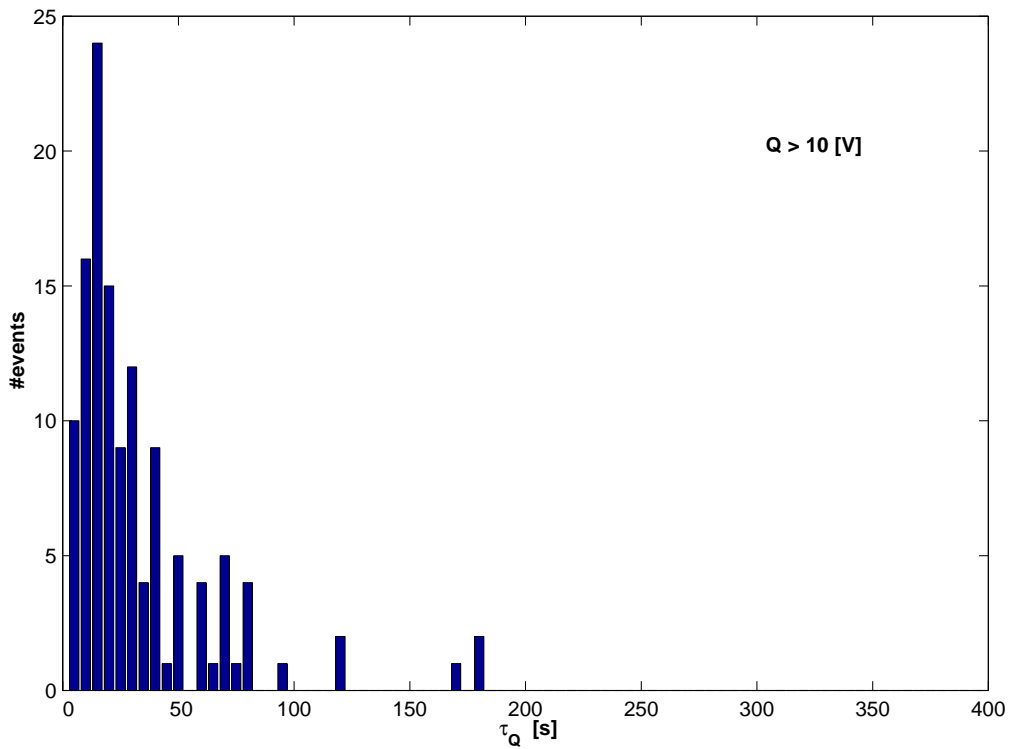


Figure 3.1.2b: Distribution of time duration of charging events (for negative charging levels in excess of -10 V). A maximum can be seen around 20 s duration.

3.2 VARIATION WITH SUNLIGHT CONDITIONS

The Freja charging events were distributed with respect to sunlight conditions according to the following:

- 32 events occurred during sunlight
- 236 events occurred during eclipse
- 23 events occurred during terminator conditions

Most Freja charging events therefore occurred during the dark winter months as can be seen in Figure 3.2.1, where the period between November and February hosts most of the Freja charging events. The sunlight events (blue or black portion at bottom of bars) are possibly more spread out over the year, but there are no events detected during the summer months, at least not over the Northern hemisphere. No data from the Southern hemisphere was included in this study.

The lack of charging events during the summer can only partly be explained by the additional photoemission current contribution Freja experiences during this sunlit portion of the year, since very active auroral conditions (large K_p index, see section 3.4 below) may cause charging even when Freja is sunlit. The total lack of charging events during the summer is probably also an effect of the increased thermal plasma densities at Freja altitudes (1000 – 1800 km) due to the enhanced ionisation by the solar UV radiation in the F-region ionosphere and the following upward ambipolar diffusion.

FREJA Charging Events during the Years 1992 – 1994

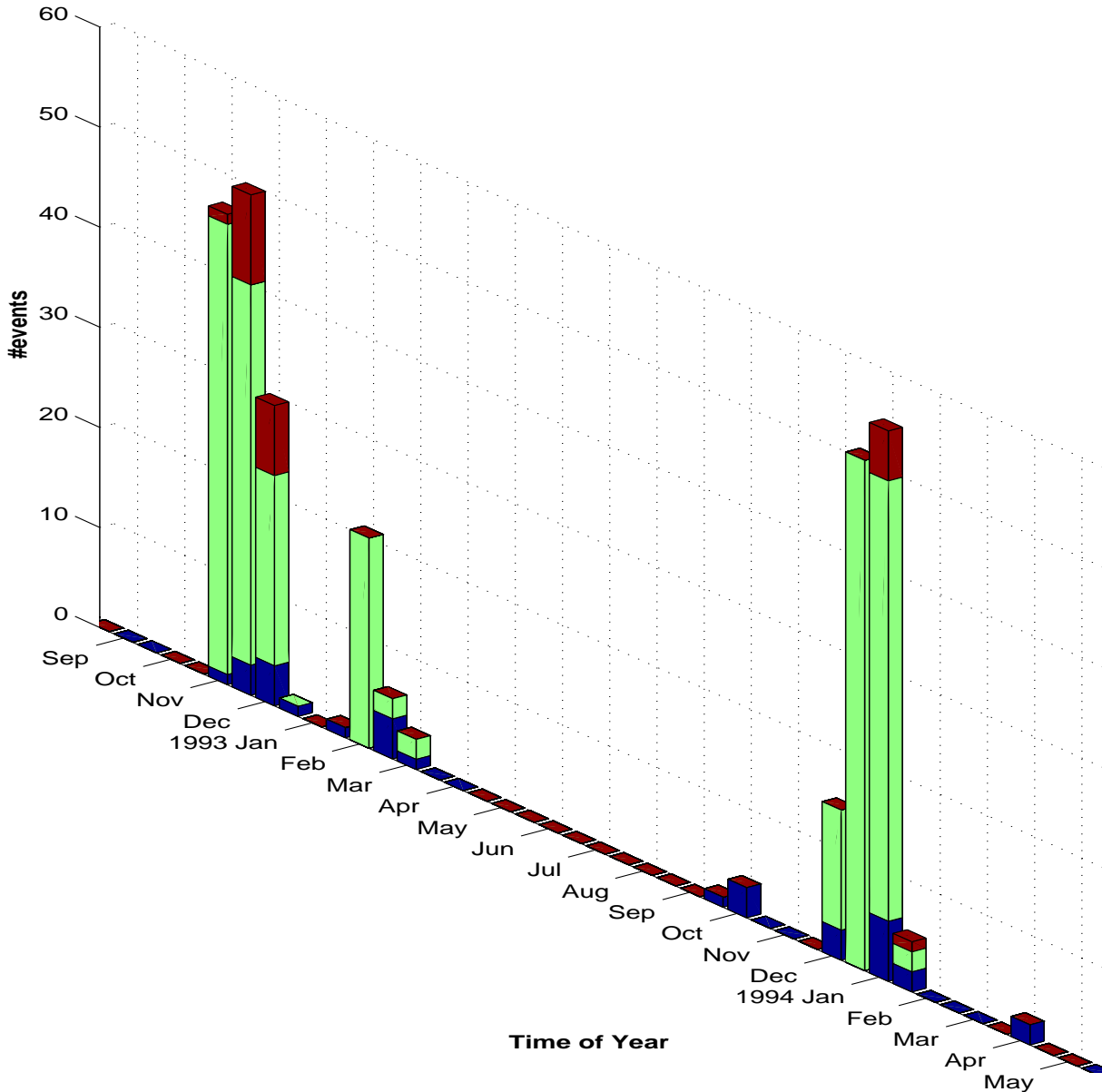


Figure 3.2.1: Distribution of charging events over the time period October, 1992, to April, 1994. The charging events dominate during eclipse (green or light grey, middle), but a few exist during sunlight (blue or black, bottom) and terminator (red or dark grey, top) conditions. No charging events exist during the summer (in these Northern hemispheric data).

3.3 VARIATION WITH GEOMAGNETIC LOCATION

The variation in Magnetic Local Time is presented in Figure 3.3.1a. Freja charging events occurs clearly during night-time hours with an event peak around 22:00-23:00 MLT. Almost no charging events exist between 06:00-18:00 MLT. Thus most charging events occur in the absence of the photoelectron emission from the spacecraft. We want to stress that this is not an artefact due to the charging events distribution in latitude or longitude (see below). This is proven by the MLT normalisation graph where only latitudes and longitudes of typical charging regions have been kept (Figure 3.3.1b). All MLT values were covered rather evenly by the Freja orbits.

FREJA Charging Events Distribution in MLT

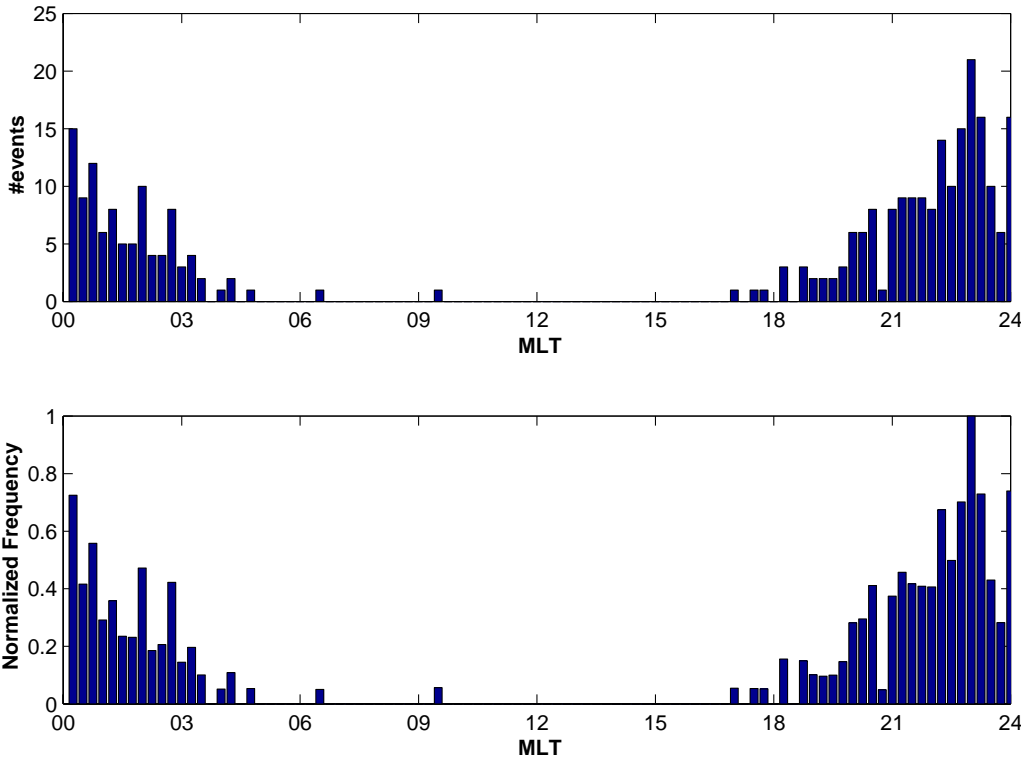


Figure 3.3.1a: Distribution of charging events in MLT. Most charging events occur in the absence of photoelectron emission in the night-side. Compare with Figure 3.2.1.
MLT Coverage of FREJA

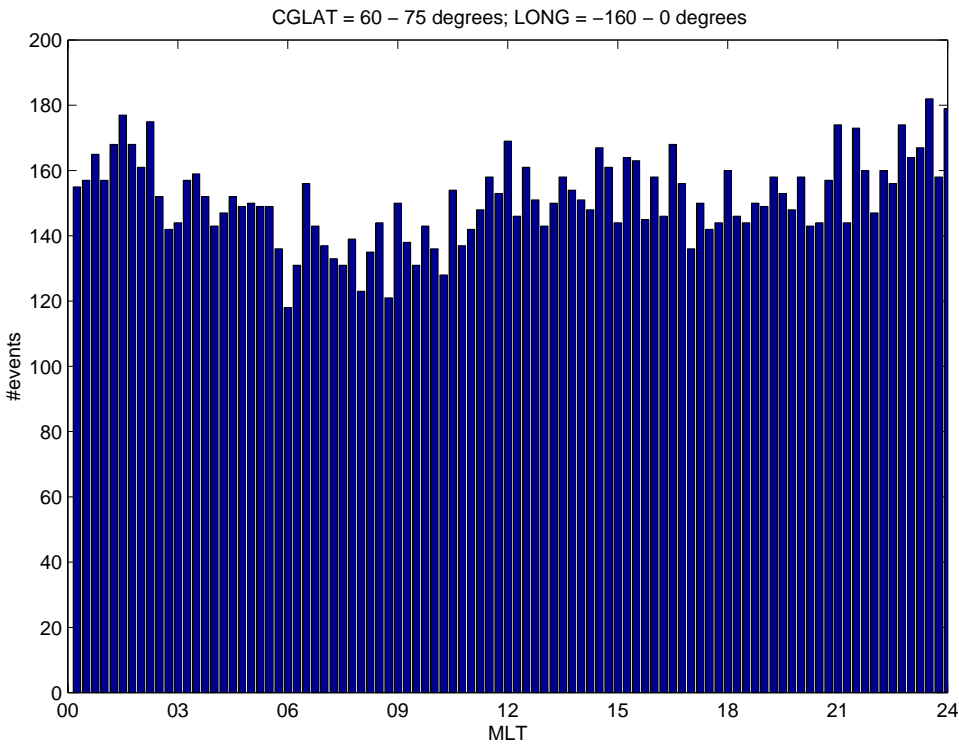


Figure 3.3.1b: Freja data taking coverage in MLT for auroral latitudes (CGLAT = 60° - 75° and Longitude = -160° - 0°).

The variation in Corrected Geomagnetic Latitude is presented in Figure 3.3.2. Freja charging events are restricted to latitudes above 60° . The charging event frequency seems to decrease at geomagnetic latitudes above 70° . Clearly, all Freja charging events occur within the auroral zone.

FREJA Charging Events Distribution in CGLat

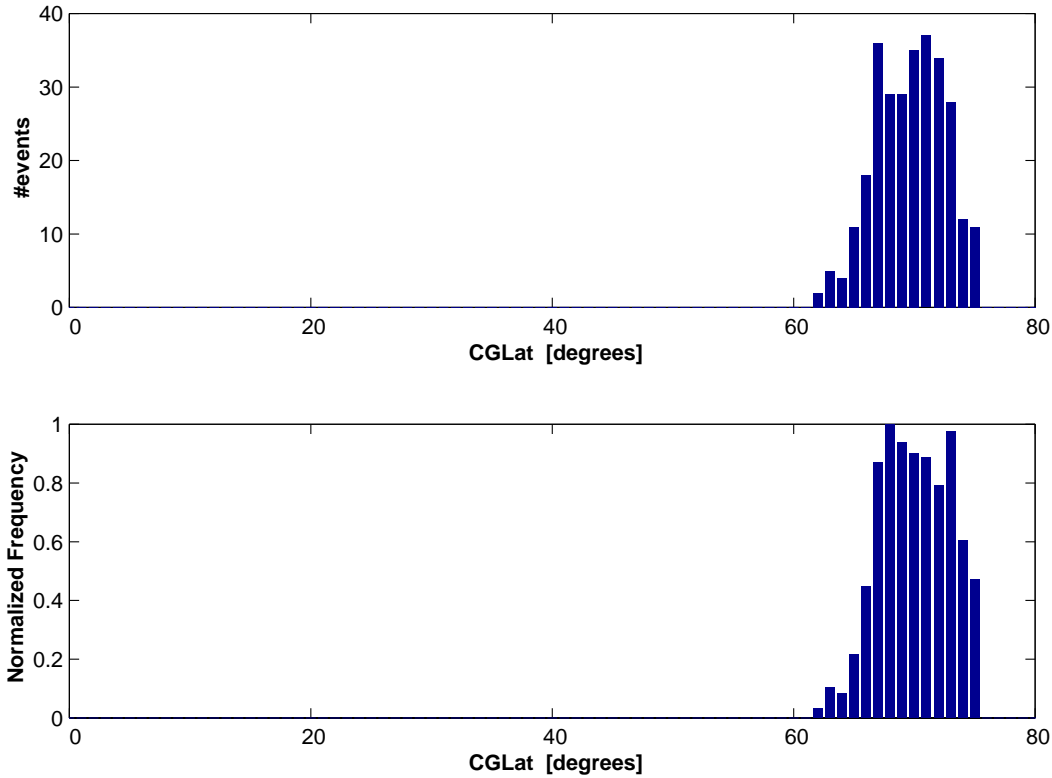


Figure 3.3.2: Distribution of charging events in CGLAT. Freja data cover $CGLAT = 35^\circ - 75^\circ$ (compare Figure 2.7.3). Charging events only occur in the auroral zone.

The variation in Longitude is presented in Figure 3.3.3. Except for the two events near -155° , the distribution is contained to -140° to -30° longitude. This is just due to a latitudinal effect as can be seen in Figure 3.3.4 where it is obvious that large enough latitudes are only reached inside this longitude range. Of course, during very active conditions (large Kp index) large fluxes of keV electron precipitation is expected within the auroral zone as will be further shown below.

FREJA Charging Events Distribution in Longitude

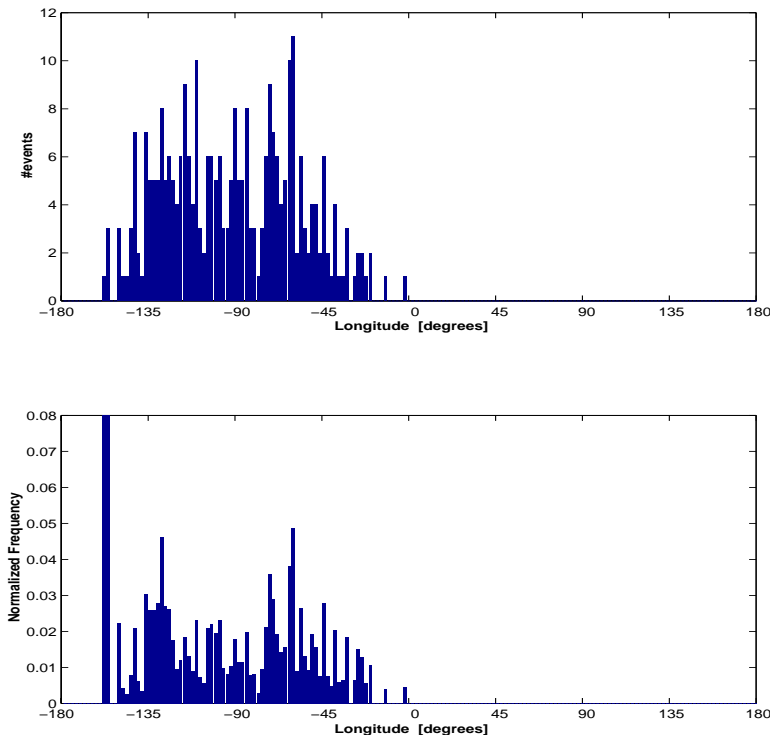


Figure 3.3.3: Distribution of charging events in Longitude. Charging events apparently occur only over Prince Albert (compare with Figure 2.7.7), which is just due to that large enough Latitudes are only reached for these Longitudes (compare with next Figure).

FREJA Charging Events, Longitude – CGLAT

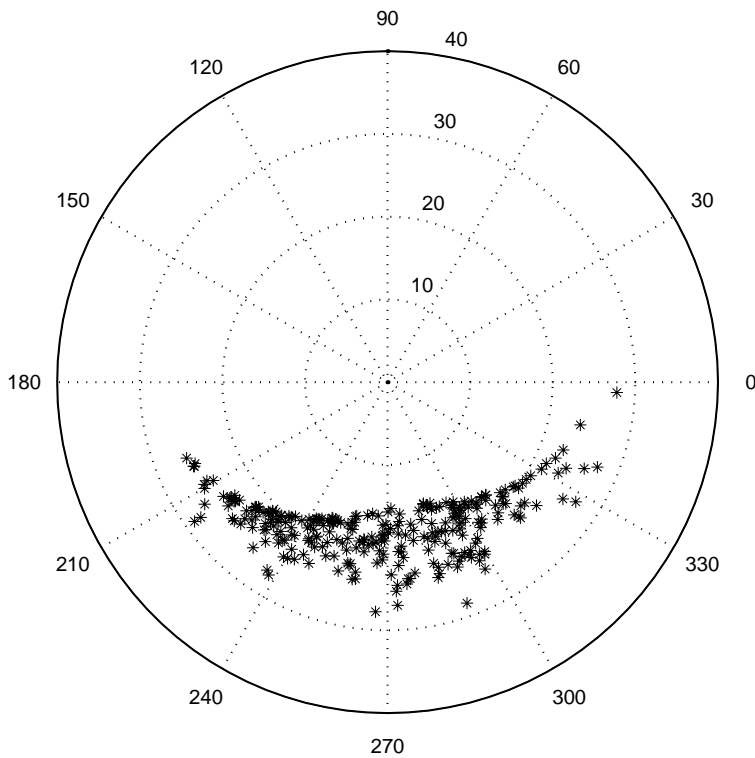


Figure 3.3.4: Charging event distribution on the northern hemisphere. The Latitude numbers are 90° - CGLAT.

3.4 VARIATION WITH GEOMAGNETIC ACTIVITY

The Freja charging events have been binned to fit the 3-hour averages of the global Kp index, an indicator for geomagnetic activity. The bottom panel of Figure 3.4.1 shows the normalisation used for the Freja time period, the middle panel shows the normalised results for the Freja charging events. We can note that

- there is a weak increasing tendency with increasing Kp indices
- the probability of charging becomes large for $Kp > 2+$.

These results agree fairly well with the results of *Mullen et al.* (1986), based on geostationary SCATHA data, while only a small correlation was obtained between Kp index and charging levels on the DMSP satellites in LEO orbit (*Frooninckx and Sojka, 1992*).

Charging events of the Freja satellite

Nov 3, 1992 – Apr 10, 1994 (Orbits 371 - 7279)

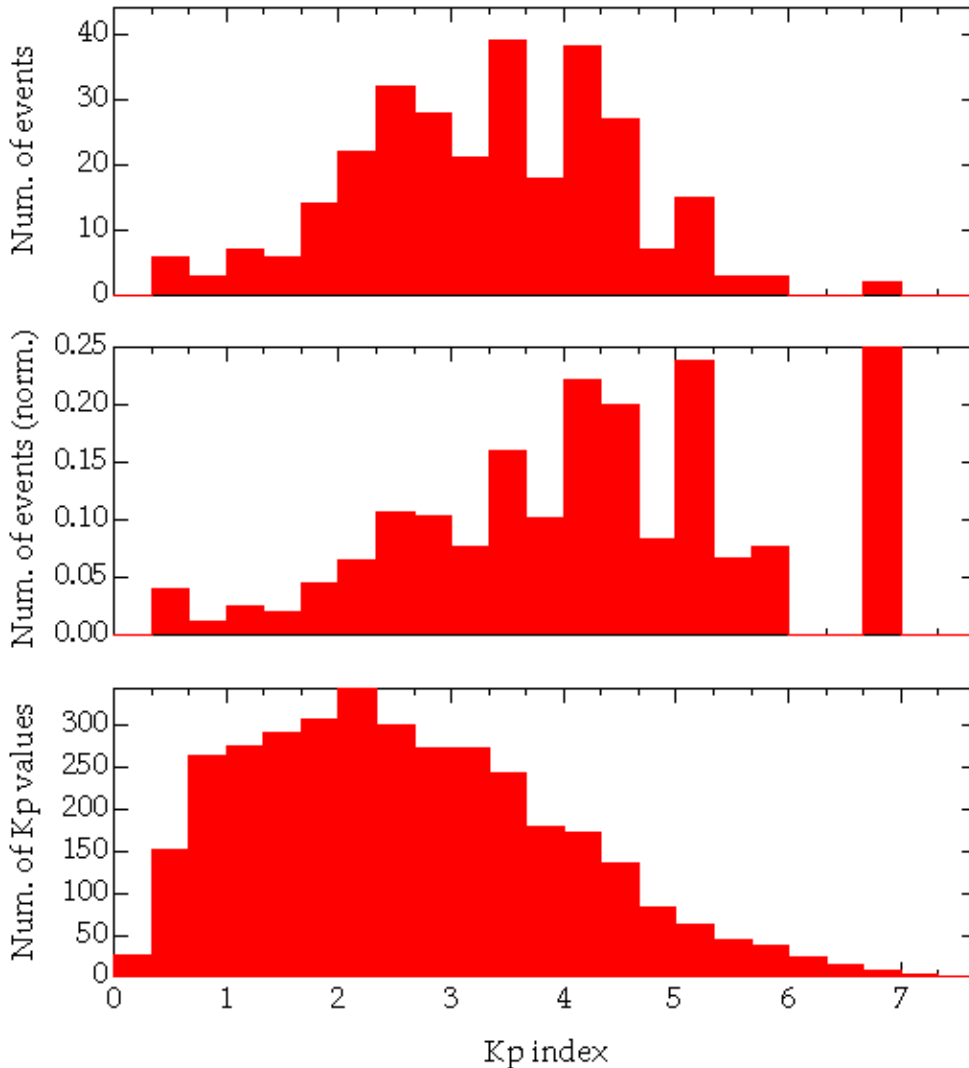


Figure 3.4.1: Dependence on the global Kp index (geomagnetic activity). The Figure display the number of charging events vs Kp index (panel a), the normalized distribution of charging events vs Kp index (panel b), and Freja Kp coverage (panel c). Charging probability increases above $Kp > 2$.

Figure 3.4.2 shows the Kp index dependence with MLT, altitude, and sunlight conditions for the Freja charging events. The data points in the eclipse index (panel c) have here been shifted randomly in order to highlight the distribution of events with sunlight conditions better. We can note that

- low Kp events tend to occur in a narrow local time sector near local midnight (panel a)
- high Kp events can happen during a broader local time sector on the nightside, although the Freja spacecraft need not be in shadow (panel a compared to panel b)
- low Kp events occur only during eclipse (panel c)
- no obvious dependence with altitude exist, even though a weak trend favours lower altitudes for larger K_p indices.

Charging events of the Freja satellite

Nov 3, 1992 – Apr 10, 1994 (Orbits 371 -7279)

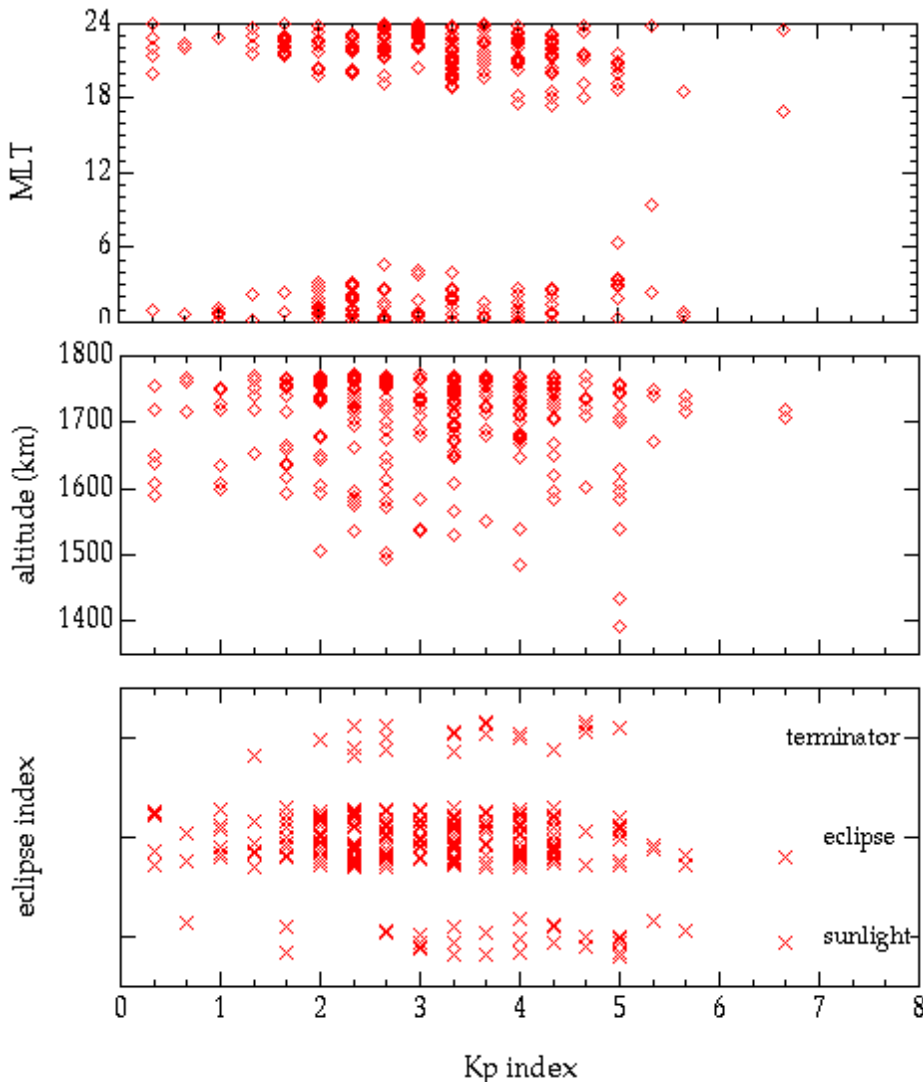


Figure 3.4.2: Dependence of the global Kp index (geomagnetic activity) for the charging events with respect to MLT (panel a), altitude (panel b), and sunlight conditions (panel c). In panel c the data have been randomised in order to highlight the distribution better. Higher geomagnetic activity level is needed for charging during sunlight conditions.

3.5 VARIATIONS WITH COLD PLASMA CHARACTERISTICS

Figure 3.5.1 (panel a) show the peak charge value variation of Freja charging events with electron density. Here, the peak charge value has been slightly randomised (10 %) to highlight the dependence better. Unfortunately no clear relationship is obvious. However, there exist an upper threshold value of $2 \cdot 10^9 \text{ m}^{-3}$ for the cold plasma density, since it is well known that the cold plasma density often reach above this value in the Freja data. The thermal plasma density seldom decrease below 10^8 m^{-3} in the Freja data set (based on Freja data analysis experience – a more comprehensive study of the plasma density and electron temperature distributions is underway).

This result can be compared with the results obtained by *Frooninckx and Sojka (1992)*, who detected a similar electron density threshold value of 10^{10} m^{-3} for the DMSP satellites. Since the DMSP satellites traversed lower altitudes (840 km) and therefore larger thermal plasma densities, this result confirms that the Freja spacecraft was indeed better designed with conductive surface coatings for electrical cleanliness. Despite this fact, Freja nevertheless charged more than 2000 Volts negative.

Density Dependence of FREJA Charging Events

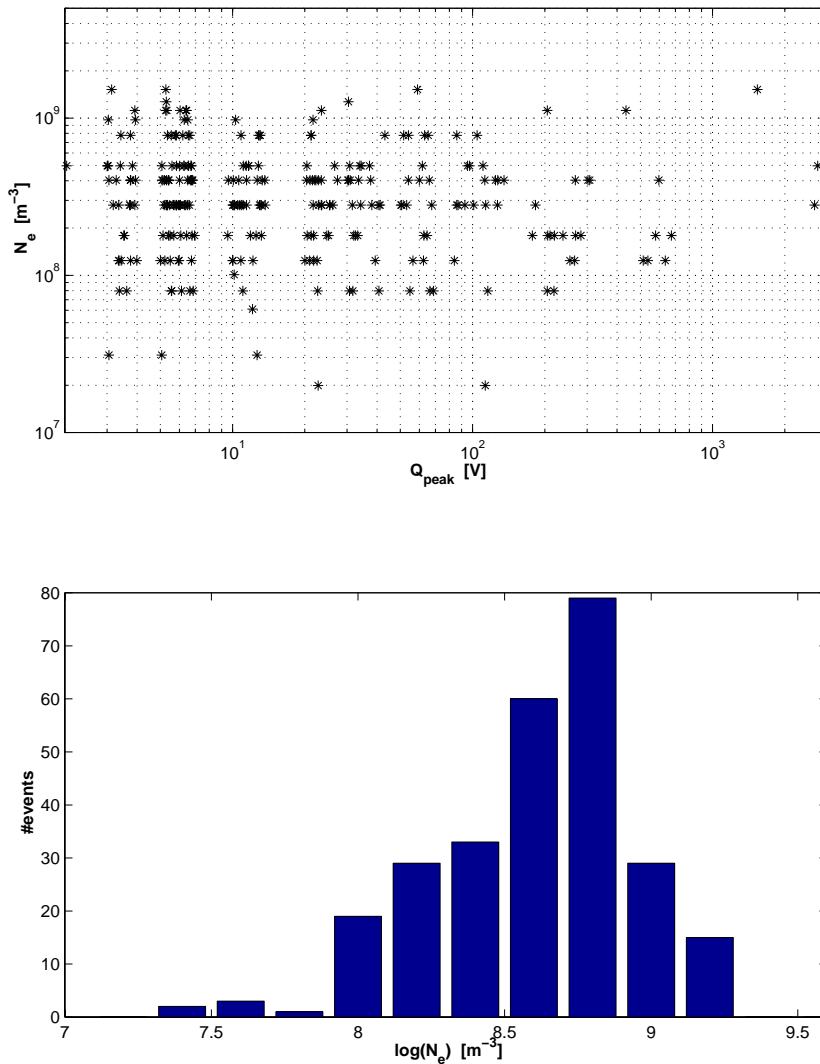


Figure 3.5.1: Charging level dependence on cold thermal plasma density. A cutoff exist around $2 \times 10^9 \text{ m}^{-3}$, above which no charging events occur. Plasma densities rarely decrease below 10^8 m^{-3} . No other obvious relationship exist between charging level and plasma density.

3.6 VARIATION WITH ENERGETIC PARTICLE CHARACTERISTICS

By far the most common type of Freja charging events is associated with energetic electron precipitation in association with so called inverted-V events. It is fair to conclude that the energetic electrons with energies above a few keV are the direct cause for most Freja charging events. Figure 3.6.1 show an averaged electron spectrum for all Freja charging events, where a clear inverted-V electron population with a peak energy of few keV (panel a) and an extended power-law type high energy tail extending to several tens of keV can be seen (panel b). Typical flux levels at the inverted-V energy peak during single charging events are most often in the range $10^6 - 10^8$ $[(\text{cm}^2\text{-s-str-keV})^{-1}]$. The TESP data are uncertain to within a factor 3, due to selected sector and geometric factor uncertainties associated with the “overview” data used for this particular statistical study.

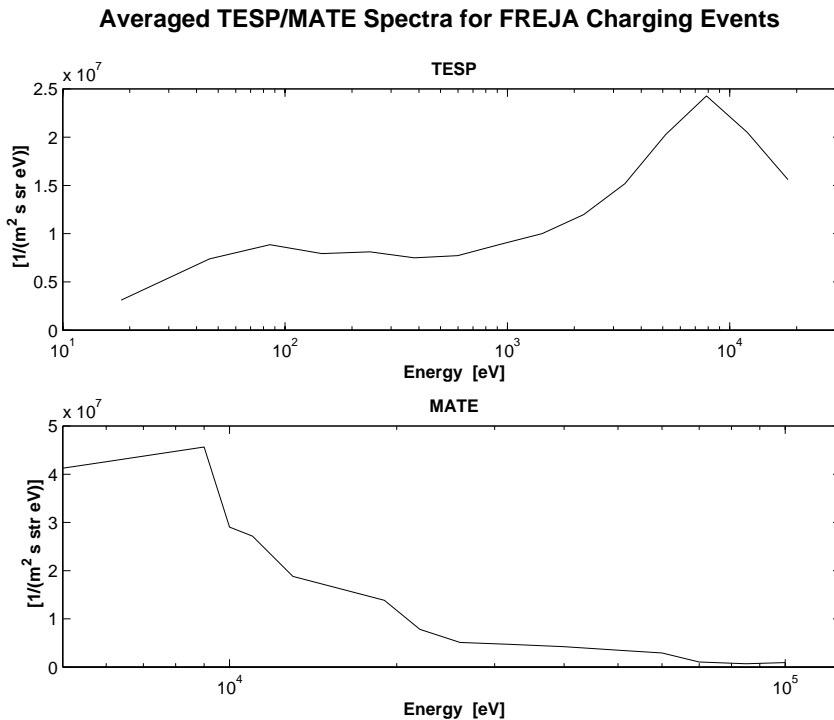


Figure 3.6.1: Averaged electron spectra for all charging events. TESP (panel a) and MATE (panel b) data reveal that auroral inverted-V type electrons with energies above a couple of keV are associated with Freja charging events. A high-energy tail in the energy range 10 - 80 keV can also be seen.

The relationship of spacecraft charging can be further demonstrated by looking at the averaged electron spectra for different charging levels (Figure 3.6.2). It is clear from Figure 3.6.2 that both the inverted-V peak energy as well as the high energy tail flux between 10 keV – 100 keV are increased for higher charging levels. Note also that no significant electron fluxes exist at lower energies (< 1 keV). Such electrons would increase the secondary yield and inhibit charging on Freja, since ITOC is the main surface coating on Freja and since ITOC has a break-even point with respect to secondary electrons near 2.5 - 3 keV [see SPEE-WP120-TN]. The second most common surface material is the thermal blanket, which has a break-even point just below 4 keV. The results are therefore in qualitative agreement with standard surface charging theory (e.g. Garrett, 1981; Hastings, 1995; Hastings and Garrett, 1996; see also SPEE-WP120-TN).

Averaged TESP & MATE Spectra for Different Charging Levels

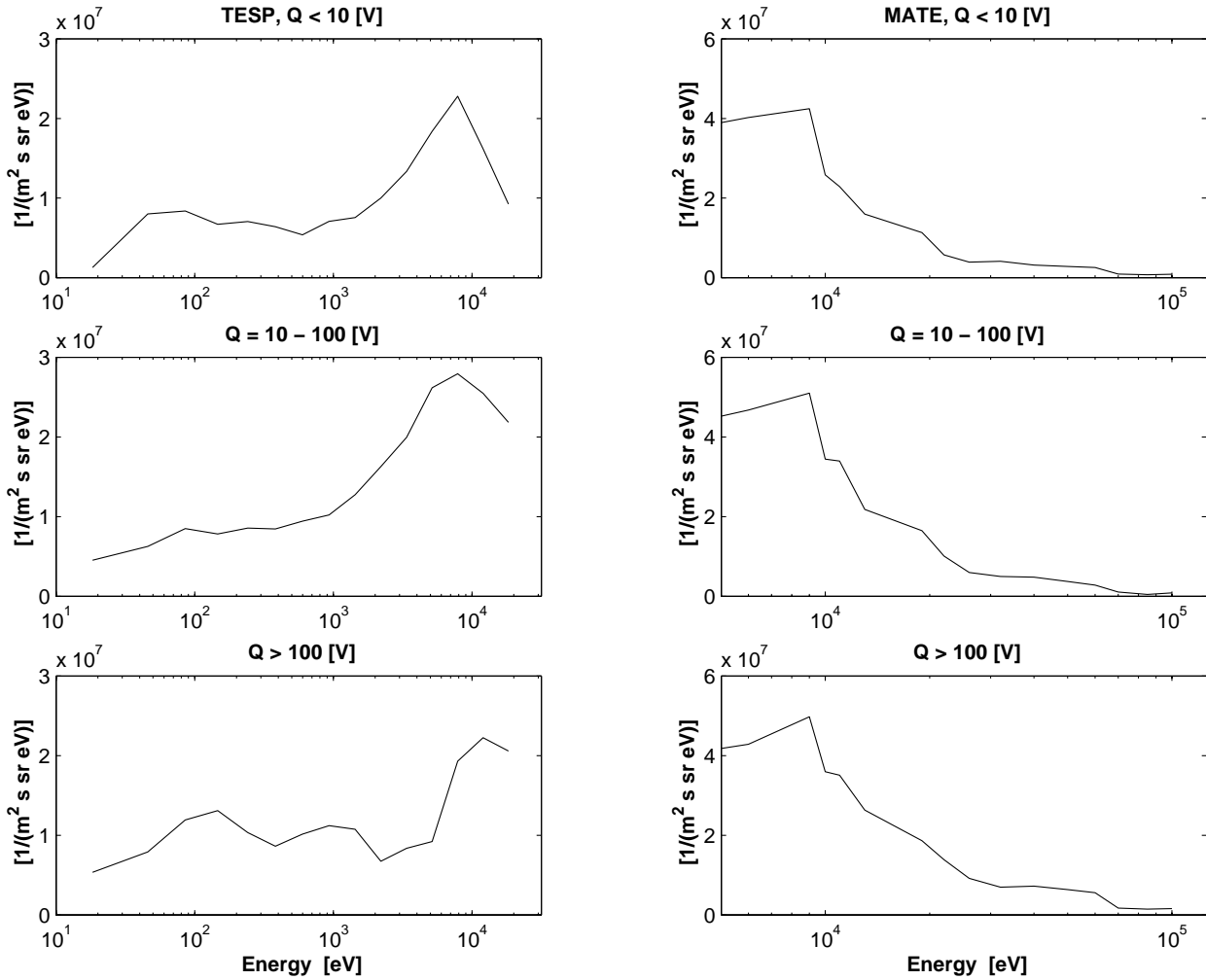


Figure 3.6.2: Averaged electron spectra for negative peak charging levels below 10 V (topmost panels), between 10 - 100 V (middle panels), and above 100 V (bottom panels). Two effects can be detected: 1) the inverted-V peak increases its energy, and 2) the high energy tail population (10 - 80 keV) is enhanced with charging level.

Frooninckx and Sojka (1992) showed that the thermal plasma density is one of the major factors determining the charging level. We show in Figure 3.6.3 the electron flux for a selected number of fixed electron energy levels (for the MATE instrument) plotted versus the peak charging level. As expected, no sensational relationship can be detected. It is obvious that the high energy electron flux *alone* is not a major physical parameter for determining the charging level of Freja. If we instead divide the flux with the cold plasma density, as Frooninckx and Sojka (1992) did, a somewhat better (still bad) relation appears. However, a somewhat better relationship is obtained near the peak energy (~10 keV) if we also divide the flux with the flux at the lowest trustable energy channel (1 keV, Figure 3.6.4). This low energy flux is well below the break-even energy for secondary electrons emitted from the surface, and the larger this flux is the lower charging level we expect. A high energy electron flux level is indeed needed, but it seems other physical parameters, such as the thermal plasma density (and the ion return current from this plasma to the spacecraft) and the low energy electron flux (which produces many secondary electrons) determines the charging level to a great extent as well. A somewhat better dependence therefore exists in Figure 3.6.4. Thus the following relationship seems to roughly hold:

$$Q \propto \left(\frac{\Phi_{peak}}{\Phi_{low} \cdot n_e} \right)^{1.5}$$

where Q is the charging level attained, n_e , the thermal plasma density, Φ_{peak} , the electron flux at the inverted-V peak energy, and Φ_{low} , the electron flux at low energies (e.g. around a few hundred eV).

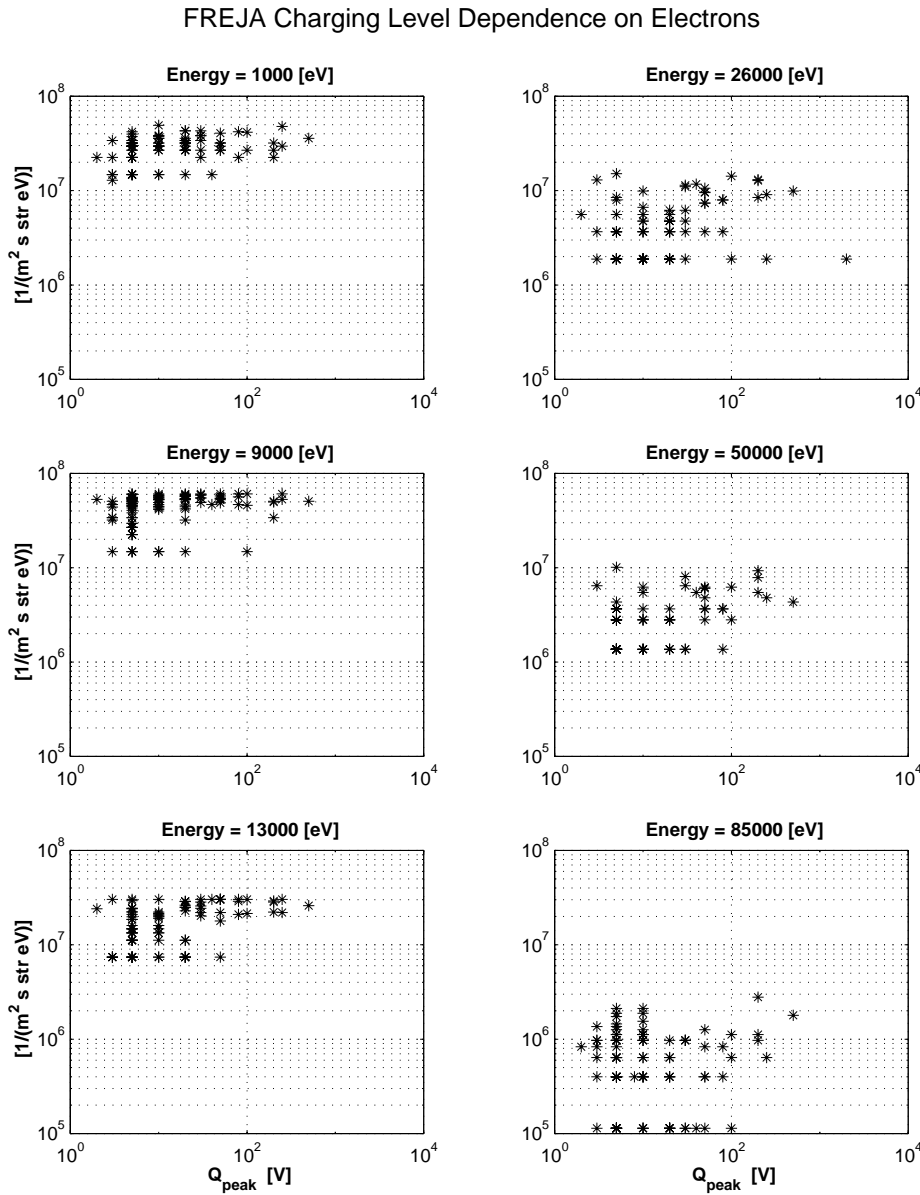


Figure 3.6.3: Dependence of electron flux with charging levels for different energies. No obvious relationship seems to exist.

FREJA Charging Level Dependence on Electrons

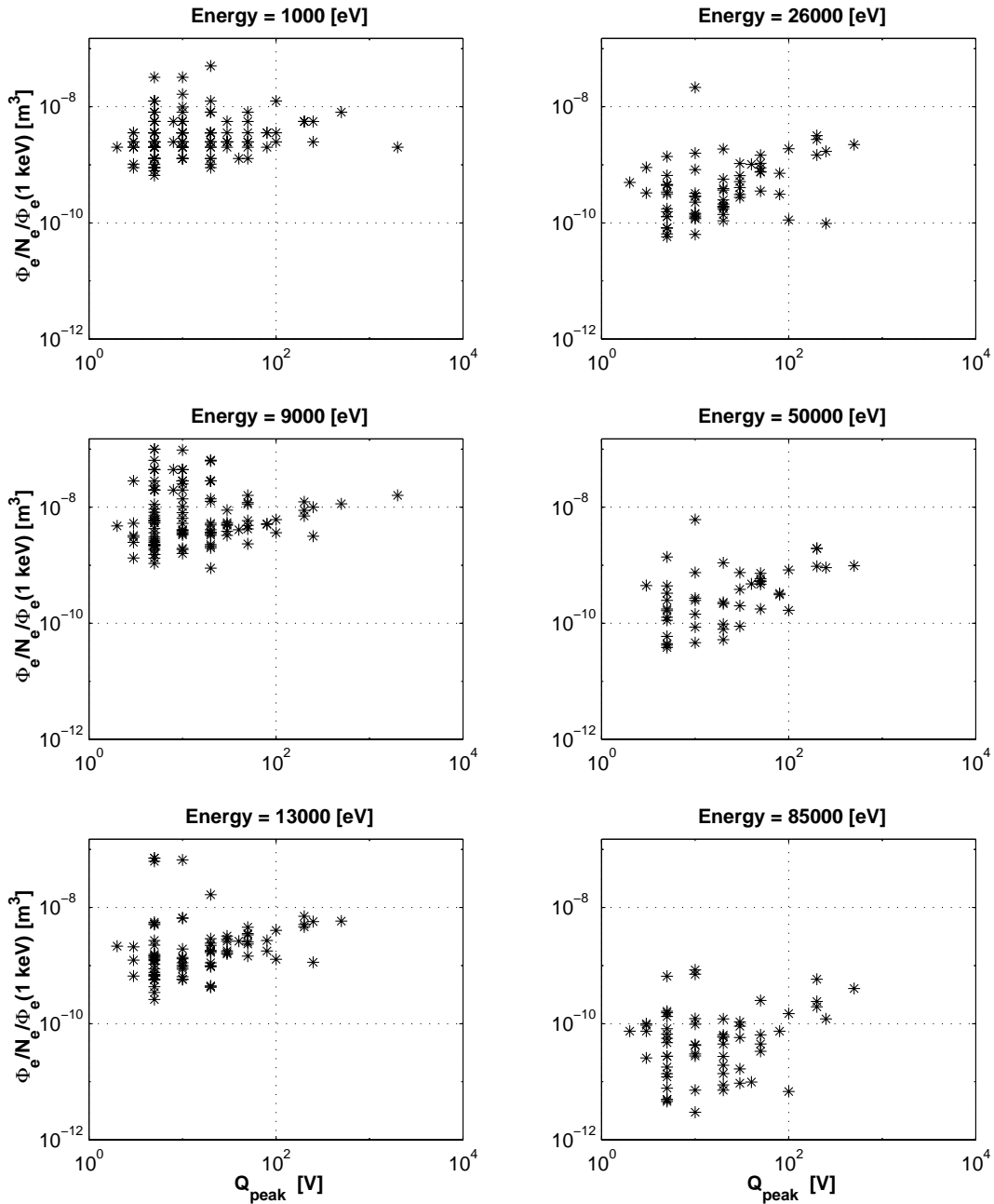


Figure 3.6.4: An increasing tendency can be found versus charging level near the inverted-V peak energy (here ~ 10 keV, plot 5) if one takes into account a combination of the total electron flux at the inverted-V energy peak (amounts of charging electrons with low secondary electron yield), the cold plasma density (ion return current to the spacecraft), and the electron flux at the lowest energy (1 keV) where the secondary electron yield is in excess of one.

3.7 VARIATION WITH ALTITUDE AND MAGNETIC FIELD STRENGTH

The distribution of Freja charging events with altitude is displayed in Figure 3.7.1. The normalised altitude occurrence of charging events (panel b, although "noisy") seems to be rather evenly distributed. Perhaps an increasing trend can be detected for increasing altitude, but this trend is within the possible errors.

In low Earth orbit, the geomagnetic field \mathbf{B} is strong enough so that secondary electrons and photoelectrons emitted from the spacecraft surface have an average gyroradius smaller than typical dimensions of a spacecraft. For Freja conditions these dimensions are comparable. This implies that escape of such electrons may be inhibited on surfaces nearly parallel with \mathbf{B} , which in turn may affect the current balance of the spacecraft and making high-voltage charging more likely (Laframboise, 1988). In the case of Freja the amount of surface parallel will be dependent on the spacecraft orientation, since Freja can be approximated by a flattened cylinder [see SPEE-WP120-TN]. We have therefore investigated the effect of the Freja orientation with respect to the magnetic field direction. Figure 3.7.2 displays the dependence of the Freja spin axis angle to the magnetic field direction. An apparent increase of charging events can be detected for smaller magnetic field angles (panel b). However, this is just a latitude effect as can be seen in Figure 2.7.11. Figure 3.7.3 further show that no obvious dependence exist between charging level and magnetic field direction in the Freja dataset. We conclude that the magnetic field orientation is not a major factor for determining charging level of the Freja satellite.

Freja Charging Events Distribution in Altitude

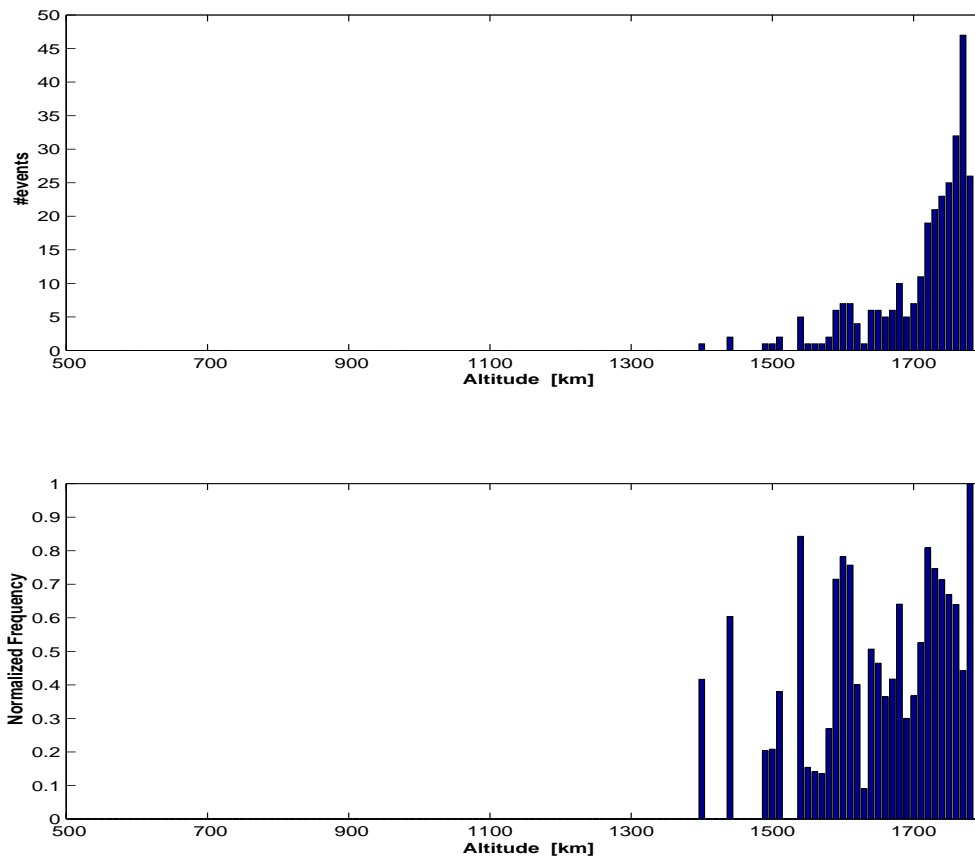


Figure 3.7.1: Distribution of charging events with altitude. The lowest charging event occurs near 1400 km, but the normalised distribution (panel b) show a rather even altitude dependence or at best a very weak increase with altitude. Freja covers altitudes down to 1000 km (compare with Figure 2.7.1).

FREJA Charging Events Distribution with Magnetic Angle

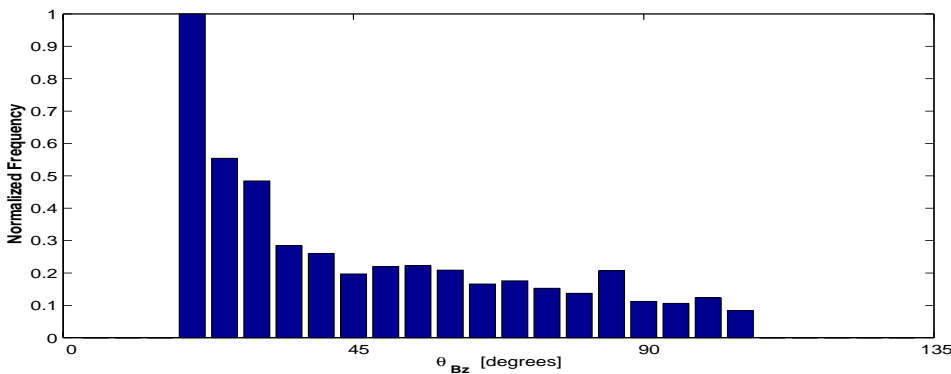
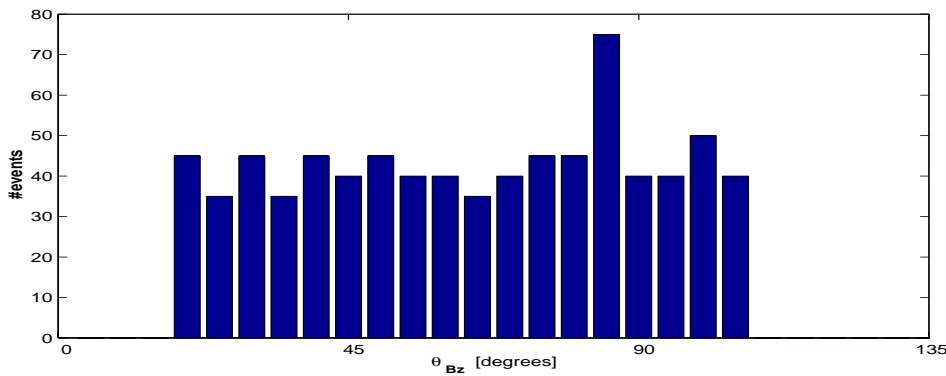


Figure 3.7.2: Dependence with spin axis angle versus the geomagnetic field (θ_{Bz}). There is an apparent increase in number of charging events for small angles. However, this effect is not real but is only a latitude effect (compare with Figure 2.7.11). Thus, no obvious dependence exist.

Peak Charge Level vs FREJA Orientation wrt Magnetic Angle

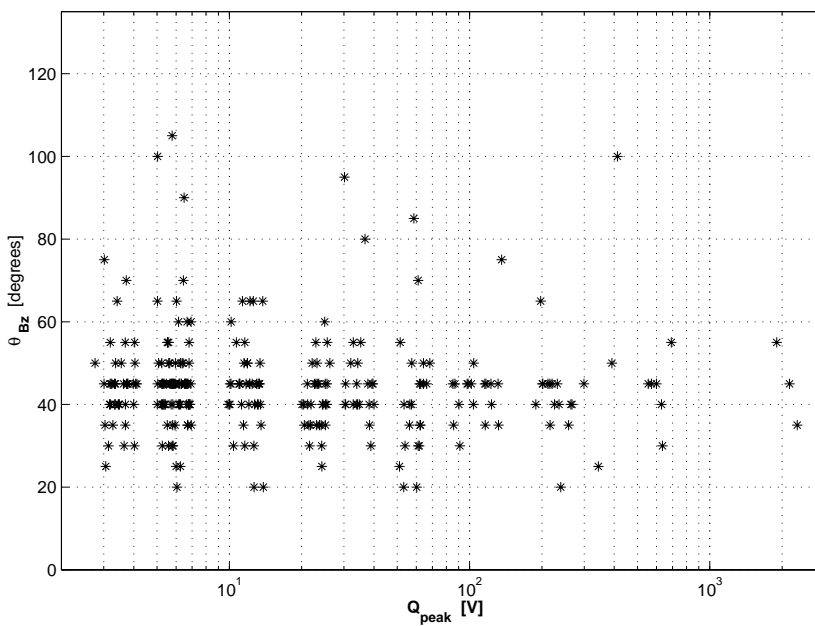


Figure 3.7.3: Dependence of charging level with spin axis angle versus the geomagnetic field (θ_{Bz}). No obvious dependence exists. Compare with previous Figure.

4. DISCUSSION OF RESULTS

4.1. CHARACTERISTICS OF FREJA CHARGING EVENTS

From a survey comprising about 2000 consecutive Freja orbits, 291 electrostatic charging events have been identified during northern high latitude passes. Four different types of charging events have been identified by the Freja plasma instruments [see SPEE-WP110-TN]:

- Charging by energetic electrons during eclipse.
- Charging by energetic electrons during sunlight and terminator conditions.
- Low level charging variations due to sunrise/sunset.
- Low level charging probably due to an increased bulk electron temperature.

The events belonging to the first category constitute by far the most common type of high level charging. The two last usually result in charging levels below the threshold we have chosen for this statistical study, and therefore only very few such events are included in this study.

Based on data sampled on 291 orbits by the Freja spacecraft within the period October-1992 to April-1994 during declining solar activity we summarise our charging observations as follows:

- The main part of the charging events did not reach charging levels in excess of 10 Volts (negative). Only a handful of the events reached charging levels around -2000 Volts.
- The duration of the charging events were mostly shorter than 1 minute. Only very few continued for several minutes even though Freja had an orbit that passed almost tangentially along the auroral oval. This fact just reflects the passage time over so called inverted-V structures within the auroral region (i.e. bursty fluxes of precipitating high energy electrons). Thus, when the source for charging disappears, the charging disappears simultaneously. This is confirmed by the results from the event study (SPEE-WP110-TN).
- All the charging events occur only above Corrected Geomagnetic Latitudes of 60° with an frequency peak centered above the auroral zone.
- The Geomagnetic activity need be larger than $K_p > 2+$ for charging events to be probable and the probability for occurrence increases for larger K_p indices.
- Typical inverted-V electron differential fluxes are $10^6 - 10^8$ (cm²-s-str-keV)⁻¹. Examples of worst case electron spectra can be found in SPEE-WP110-TN. However, the ambient plasma density, sunlight conditions and the energy of the inverted-V peak affect the charging levels more dramatically. Also, the electron flux at a few hundred eV, where the surface secondary yield is larger, was suggested to inhibit negative charging.
- No Freja charging events occurred for thermal plasma densities above $2 \cdot 10^9$ m⁻³. DMSP had a threshold value of 10^{10} m⁻³. The larger density increases the neutralising thermal ion return current to the spacecraft.
- The electron spectra show low flux levels below about 1 keV, and larger flux levels above a few keV. The spectra seem to have two populations, one with peak energies of a few keV, and one high energy tail between 10-100 keV.
- Most charging events occurred during the absence of photoemission from the Freja spacecraft (i.e. in eclipse), and enhanced negative charging levels were obtained during sunlight only for very active auroral conditions ($K_p > 2-3$).
- No charging events occurred during the summer months, while a maximum occurred in the winter months. This behaviour is most probably due to the combined effect of sunlight (photoelectron emissions) and the expected larger thermal plasma densities due to upward diffusion from the stronger ionospheric F2 layer during the summer months.
- Most charging occurred in the MLT interval 18 pm – 03 am.

- No obvious relationship was detected regarding the orientation of the Freja spin axis with respect to the geomagnetic field direction even though the electron gyroradius of the photoelectrons and secondary electron emission from the spacecraft surface and the dimensions of Freja are comparable.

We therefore conclude that high level negative charging (of several tens of Volts to thousands of Volts) on the Freja spacecraft is caused by the energetic electron precipitation in connection with high-latitude auroral inverted-V events with peak energies above a few keV. Worst case events can be found in SPEE-WP110-TN.

4.2. COMPARISON WITH DMSP STATISTICS

The results from this study can be compared with the Defence Meteorological Satellite Program (DMSP) statistical results obtained from the somewhat lower altitude of 840 km [e.g., *Gussenhoven et al.*, 1985; *Yeh and Gussenhoven*, 1987; *Frooninckx and Sojka*, 1992; and *Stevens and Jones*, 1995]. A summary of the DMSP results is given in SPEE-WP110-TN (pages 7 – 8).

The DMSP data revealed 184 events of negative surface charging in the range –47 to –1430 V during periods of intense energetic electron precipitation within the auroral region. The charging events onboard the DMSP spacecraft is therefore most probably of the same type as those detected onboard Freja. However, there are a few observational facts that distinguish the Freja results from the DMSP results:

- All the DMSP charging events occurred during eclipse [*Gussenhoven*, private communication 1998; *Gussenhoven et al.*, 1985], while the Freja data set contained a few events during sunlight or terminator conditions. This may be due to that Freja encountered more intense precipitation events and lower plasma densities such that the balancing effect of photoelectron emissions could not prohibit surface charging.
- The DMSP charging events were co-located with plasma depletions [e.g. *Gussenhoven et al.*, 1985], while the Freja results indicate that thermal plasma density is often largely unaffected. Instead the Freja results show that certain instruments relying on direct measurements of the electrical properties of the surrounding plasma to determine the plasma density (like a Langmuir probe instrument) are affected by measurement artefacts caused by the charge state of the spacecraft itself. The SSIE instrument used for plasma density estimates onboard DMSP might have been affected in a similar way as the Langmuir probe did onboard Freja.
- Electrons with as low energy as 2-3 keV contributed to charging onboard DMSP [*Frooninckx and Sojka*, 1992], while energies above 5 keV was necessary to charge Freja. Also, the upper threshold plasma density making surface charging possible onboard DMSP was about 10^{10} m^{-3} , while Freja threshold was a factor five lower ($2 \cdot 10^9 \text{ m}^{-3}$). This probably just reflects the better surface material properties of Freja with respect to charging.

5. CONCLUSIONS & GUIDELINES FOR FUTURE MISSIONS

It is worrisome that a spacecraft devoted to the scientific investigation of auroral processes, including the measurement of charged particles at low energy, occasionally gains charging levels of several thousand volts negative during auroral active conditions. Freja was a spacecraft where the designers had made special care to provide conductive surfaces of high secondary electron emission material, mainly Indium Tin Oxide (ITO), yet high level charging appears which may cause not only electrical problems but also erosion of the surface due to sputtering by the very reactive O^+ ions encountered at low altitude (≤ 4000 km). ITOC (conductive Indium Tin Oxide Coating) has a cross over energy of about 2.5 - 3 keV, above where the secondary yield falls below 1. The second most common surface material is the thermal blankets with a slightly larger secondary yield crossover energy of just below 4 keV. The spectral characteristics of a typical auroral inverted-V events with insignificant low-energy fluxes (< 1 keV) and large fluxes of high energy electrons (often isotropic in pitch-angle) make these events especially effective in producing high charging levels on *any spacecraft* where the secondary yield crossover energy for the surface material is a few keV. Highly conductive surface materials are needed to avoid differential charging problems among different surfaces on a spacecraft. To avoid high level charging of a polar spacecraft, surface materials with secondary yield crossover energies of the order of 10 keV are needed. This is a possible challenge for material science research.

The gyroradius at Freja/DMSP altitudes for around 2 eV secondary electrons are 0.1 - 0.4 m, which is still a significant fraction of the size of Freja. Even so, only a fraction of these electrons will return to Freja through gyromotion, depending on orientation with respect to the Earth's magnetic field direction [Laframboise, 1988]. For a larger spacecraft a larger fraction of these secondaries will return to the spacecraft surface, and a larger spacecraft will therefore likely gain somewhat higher charging levels. The same argument is true with regard to sunlight conditions, when large amounts of photoelectrons are emitted from the surface. A smaller spacecraft will not see the photoelectrons return as easily as a larger spacecraft, and the larger spacecraft is therefore more easily charged.

The time duration of the Freja charging events reflects exactly the presence (time duration) of the energetic electron precipitation of the inverted-V events. Thus, when the source for charging disappears, the charging disappears simultaneously. We therefore suspect that very little differential charging between different Freja surfaces occurred, which is confirmed by the POLAR simulations (see SPEE-WP120-TN).

High level surface charging is likely to continue to occur on spacecrafts in PEO/LEO. Unless serious engineering efforts are made to produce surface materials with large secondary yields for incident electron energies in excess of tens of keV, and which are still conductive, it will not be possible to protect spacecrafts completely from long term degradation. An alternative is to avoid sending spacecrafts into the auroral or similar environments. Active methods to reduce charging levels exist, like expelling a cold rather dense plasma around the spacecraft, but such methods instead may increase the contamination and differential charging problems. Problems which will affect the performances of scientific instruments onboard these spacecrafts, but also navigation systems like star trackers.

6. REFERENCES

- Anderson, P. C., and H. C. Koons, Spacecraft charging anomaly on a low-altitude satellite in an aurora, *J. Spacecraft and Rockets*, vol. 33, no. 5, 1996.
- Carruth, M. R., and M. E. Brady, Measurement of the charge-exchange plasma flow from an ion thruster, *J. Spacecraft Rockets*, 18(5), 457-461, 1981.
- Dettleff, G., Plume flow and impingement in space technology, *Prog. Aerospace Sci.*, 77, 3587-3611, 1991.
- Frooninckx, T. B., and J. J. Sojka, Solar cycle dependence of spacecraft charging in low earth orbit, *J. Geophys. Res.*, vol. 97, no. A3, pp 2985, 1992.
- Garrett, H. B., The charging of spacecraft surfaces, *Rev. Geophys. Space Phys.*, vol. 19, no. 4, pp 577, 1981.
- Garrett, H. B., and C. P. Pine, Eds., *Space systems and their interactions with earth's space environment*, vol. 71, *Progress in Astronautics and Aeronautics Series*, American Institute of Aeronautics and Astronautics, New York, 1980.
- Gussenhoven, M. S., D. A. Hardy, F. Rich, and W. J. Burke, and H.-C. Yeh, High-level spacecraft charging in the low-altitude polar auroral environment, *J. Geophys. Res.* vol. 90, no. A11, pp 11009, 1985.
- Hastings, D. E., A review of plasma interactions with spacecraft in low Earth orbit, *J. Geophys. Res.*, vol. 100, no. A8, pp 14457, 1995.
- Hastings, D., and H. Garret, Eds., *Spacecraft environment interactions*, Cambridge University Press, *Atmospheric and Space Science Series*, 1996.
- Koons, H. C., and D. J. Gorney, Relationship between electrostatic discharges on spacecraft P78-2 and the electron environment, *J. Spacecraft*, vol. 28, no. 6, 1991.
- Laframboise, J. G., Calculation of escape currents of electrons emitted from negatively charged spacecraft surfaces in a magnetic field, *J. Geophys. Res.*, vol. 93, no. A3, pp 1933, 1988.
- Leach, R. D., and M. B. Alexander, Failures and anomalies attributed to spacecraft charging, NASA Reference Publication 1375, 1995.
- Lundin, R., G. Haerendel, and S. Grahn, .Eds., *The Freja mission*, *Space Science Reviews*, vol. 70, Nos. 3-4, 1994.
- Mullen, E. G., M. S. Gussenhoven, D. A. Hardy, T. A. Aggson, B. G. Ledley, and E. Whipple, SCATHA survey of high-level spacecraft charging in sunlight, *J. Geophys. Res.*, vol. 91, no. A2, pp 1474, 1986.
- Newell, P. T., Review of critical ionization velocity effect in space, *Rev. Geophys. Res.*, 23, 93-104, 1985.
- Olsen, R. C., A threshold effect for spacecraft charging, *J. Geophys. Res.*, vol. 88, no. A1, pp 493, 1983.
- Rosen, A., *Spacecraft charging by magnetospheric plasmas*, American Institute of Aeronautics and Astronautics, Washington DC, 1976.

Stevens, N. J., and M. R. Jones, Comparison of auroral charging predictions to DMSP data, AIAA 95-0370, 33rd Aerospace Sciences Meeting and Exhibit, January 9-12, 1995.

Yeh, H.-C., and M. S. Gussenhoven, The statistical electron environment for defence meteorological satellite program eclipse charging, *J. Geophys. Res.*, vol. 92, no. A7, pp 7705, 1987.